5-2-2018

SPATIOTEMPORAL VARIATION OF LAND-USE AND LAND-COVER IN THE NAIROBI RIVER WATERSHED, AND ITS EFFECTS ON THE INORGANIC GEOCHEMISTRY OF NAIROBI RIVER

FRANCIS MUCHEMI

SPATIOTEMPORAL VARIATION OF LAND-USE AND LAND-COVER IN THE NAIROBI RIVER WATERSHED, AND ITS EFFECTS ON THE INORGANIC GEOCHEMISTRY OF NAIROBI RIVER

by

FRANCIS MUCHEMI

Under the Direction of Daniel M. Deocampo, PhD

ABSTRACT

Determining the effects of LULC and development on natural resources is necessary for sustainability. This study focused on LULC changes in NRW over the past 3 decades and the effects it had on the geochemistry of NR channel's sediment. Impervious surfaces increased from 2.5% to 11.9%. Samples from the urban class had elevated levels of contaminants than other classes. The concentrations of major inorganic elements were normal compared to the juvenile UCC except MnO and P_2O_5 that were heterogeneously distributed and significantly enriched. Heavy metals exhibited high DR than USEPA SSL in urban. Pb, Ce and Sb had the highest concentration of 3400, 769 and 187.5 ppm respectively in the urban class. Heterogeneously distributed and enriched elements like Pb, Y, Yb, Zr, Er,Ce, Zn, Lu, Sm, Th, Nd etc., were attributed to humans' input. Minerals identified were smectite, kaolinite, quartz, anorthoclase and critobalite? Sediments' alteration decreased down the river gradient.

INDEX WORDS: Nairobi River Watershed, Land-use and Land-cover, Geochemistry, Remote Sensing, GIS, Mineralogy

SPATIOTEMPORAL VARIATION OF LAND-USE AND LAND-COVER IN THE NAIROBI RIVER WATERSHED, AND ITS AFFECTS ON THE INORGANIC GEOCHEMISTRY OF NAIROBI RIVER

by

FRANCIS MUCHEMI

A Thesis Submitted in Partial Fulfillment of the Requirements for the Degree of

Master of Science

in the College of Arts and Sciences

Georgia State University

2018

SPATIOTEMPORAL VARIATION OF LAND-USE AND LAND-COVER IN THE NAIROBI RIVER WATERSHED, AND ITS AFFECTS ON THE INORGANIC GEOCHEMISTRY OF NAIROBI RIVER

by

FRANCIS MUCHEMI

Committee Chair: Daniel Deocampo

Committee: Crawford Elliot

Lawrence Kiage

Electronic Version Approved:

Office of Graduate Studies

College of Arts and Sciences

Georgia State University

May 2018

DEDICATION

I dedicate this thesis to my wife, Joyce and my two lovely daughters Shemmy and Stacy for being very patient with me for almost two years when I was out pursuing my M. Sc. Studies.

ACKNOWLEDGEMENTS

To start with, I would like to express my heartfelt gratitude to my thesis advisor Prof. Daniel Deocampo for the immense support he accorded me to be able to complete this thesis research. I relied on his guidance, motivation, patience, and knowledge at all times to write this thesis. Dr. Deocampo also offered me a graduate research assistant opportunity that allowed me to sail through my four semesters on Campus with a lot of ease. I would not have envisaged having a better mentor and advisor for my M. Sc. studies.

Besides my advisor, I sincerely thank the rest of my thesis committee; Prof. Lawrence Kiage and Prof. Crawford Elliott for their dedicated and insightful contributions and moral support. I also want to thank Prof. Dajun Dai for the excellent assistance in watershed delineation and analysis work. My sincere gratitude goes to the Department of Geosciences, Georgia States University for offering me a graduate teaching assistance opportunity that also facilitated my four semesters on Campus.

I appreciate and acknowledge the opportunity given to me by the National Museums of Kenya for allowing me to be out to study on a two years' study leave.

I also want to thank my fellow course mates who contributed in one way or the other to the completion of this thesis. Many thanks to my office mate Benjamin Opiyo for being a 'brother' during all that time, Nathan Rabideaux, David Davis, Lanier Henson, Vicky Cheruiyot, Alireza Namayander, and Abdulkabir Adekunle. Your assistance was recognized and highly appreciated.

TABLE OF CONTENTS

LIST OF TABLES

LIST OF FIGURES

LIST OF ABBREVIATIONS

CIA – Chemical Index of Alteration
DEM – Digital Elevation Model
DR – Detection Ratio
GIS – Geographic Information System
HREE – Heavy Rare Earth Elements
ICP-AES – Inductively Coupled Plasma Atomic Emission Spectroscopy
ICP-MS - Inductively Coupled Plasma Mass Spectrometry
LOI – Loss on Ignition
LREE – Light Rare Earth Elements
LTV – Long-term Trigger Value
LULC – Land-use and Land-cover
Ma – Million years ago
MR – Mathare River
NR – Nairobi River
NRBP – Nairobi River Basin Rehabilitation Program
NRW – Nairobi River Watershed
OLI – Operational Land Imager
PPM – Parts Per Million
REE – Rare Earth Elements
RS - Remote Sensing
SSL – Soil Screening Levels
STV – Short-term Trigger Value
TM – Thematic Imager
UCC - Upper Continental Crust
USEPA – United State Environmental Protection Agency
USGS – United States Geological Survey
WHO – World Health Organization
XRD – X-ray Diffractometer

1 INTRODUCTION

1.1 Literature Review

Human population growth in urban environments, economic development, and demand for growing need for food, water, and other basic needs has grown considerably. As a result, surface and ground water have suffered immensely from pollution and excessive withdrawals emanating from urban and agricultural areas (Shabnam et al., 2017). Both ground and surface water resources are contaminated by pollutants associated with humans and animal fecal wastes, industrial chemicals and other anthropogenic activities. Pathogenic microorganisms breed in these waters and can cause risks to human health and water impairment especially in the tropics where conditions favor the growth of microorganisms (Savichtcheva and Okabe, 2006; Tallon et al., 2005).

1.1.1 Land-use and Land-cover

Understanding the effects of land-use and land-cover (LULC) on the quality of water in a watershed, as well as detecting spatiotemporal changes of LULC is important for watershed management. Information on LULC in a watershed and its dynamics is essential in providing bases upon which decisions concerning watershed management can be anchored (Alphan, 2003). Urbanization results in building of infrastructure like roads and industries that is meant to support social-economical activities and thus increases the development of impervious surfaces on the landscape (United Nations, 2017). These impermeable surfaces affect the quality of water, public health, habitats, aquatic ecosystems, and reduce esthetic value of water in a watershed by altering runoff (Uygun and Aldek, 2015; Schueler, 1994)). Runoff from urban areas and agricultural lands may cause severe effects on downstream environment by contributing non-point source pollution. This has become a priority in monitoring, prevention, and restoration of surface water quality in many countries (Alvarez-Cobelas et al., 2008; Turner et al., 1993). Impervious surfaces aggravate

the flow of polluted runoff into the waterbodies through a network of channels and pipes (Arnold and Gibbons,1996). Remote Sensing (RS) is a technology utilized to determine spatiotemporal LULC (Foody, 2002), while Geographic Information System (GIS) is a flexible tool for collection, storage, display and analysis of digital data required for landscapes' classification and change detection (Demers, 2005). The popularity of RS and GIS technologies have led to an increase in studies focusing on quality and pollution of water, including mapping, modeling pollution sources, drinking water quality and assessing water pollution levels (Coskun et al., 2008; Foster et al., 2000).

Human/nature interaction has resulted in deforestation, increased sedimentation, reduction in net primary productivity and reduced soil quality all on a backdrop of climate change (Dwivedi et al., 2005). To better understand these processes, remote sensing images from satellite can be used to classify LULC properties in a watershed. Land-use in remote sensing is different from land-cover, and is defined as activities applied by humans on the land (Cihlar and Jansen, 2001). Mixing of land-cover and land-use in remote sensing is common for environmental assessments (Jansen and Di Gregorio, 2002). Multi-temporal and multispectral satellite images are analyzed and converted into spatiotemporal information, vital for understanding and evaluating development processes and patterns for developing LULC datasets (Steininger, 1996). Different classification methods are used in which pixels are grouped into related spectral classes by clustering algorithms. ERDAS-ERDAS imagine is a remote sensing image processing software that uses both supervised and unsupervised classification systems to classify digital images, with the later applying iterative self-organizing data analysis technique (ISODATA). ISODATA clusters pixels using iteration whereby, it recalculates the average and cluster pixels according to new mean after every iteration. The reflectance of pixels is analyzed by maximum likelihood

classification in which pixels with maximum likelihood are grouped into corresponding classes. However, there is often misclassification and inaccuracy of digital images when using automatic classification, especially when dealing with arid and heterogeneous landscapes. This inaccuracy is caused by inter-annual variability of climate, resulting to a variety of spatial patterns, variable vegetation cover, and high fragmentation (Barkhordari and Viardanian, 2012).

1.1.2 Geochemistry

Diffuse urban effluent via storm water and uncontrolled discharge of wastewater are the primary causes of surface water contamination (Defra, 2012). Clays and soils can sorb cations of many elements and compounds because most of them have surface charge. The presence of heavy metals therefore in the bottom sediments of a river reveal a history of pollution either from a human source or natural origin. This study determined the concentrations of major elements of the Earth's crust from Nairobi River, heavy metals of concern and other trace elements. Heavy metals occur naturally at a low level but may escalate to high concentrations because of anthropogenic activities such as sewage, irrigation, mining and smelting (Niu et al., 2013). Potassium (K) and Orthophosphate (PO_4) ratios, ammonia concentration above 0.3 mg/L and boron (B) ion concentration above 1.0mg/L are indicators of gray water in surface water bodies (Panasiuk et al., 2015). Heavy metals are usually considered ecologically toxic, persistent and bioavailable contaminants because they are health hazards to animals, trees and the ecosystems (Zhang et al., 2015).

The presence of arsenic (As) in surface water may be contributed by groundwater sources linked to geological sources. Arsenic is responsible for hyperkeratosis and vascular diseases in humans. Arsenic gets into the air from volcanic activities, wind erosion, volatilization from soil, and anthropogenic pollution through fossil fuel combustion and smelting (Cullen and Reimer,

1989). About 18,800 tons of As per year which is about 30% of the global total As into the atmosphere is as a result of human activities (Nriagu and Pacyna, 1988). Cadmium is spread into the air by anthropogenic activities of mining and smelting, as well as usage of phosphate fertilizers, sewage, and other industrial usages like manufacturing of batteries, pigments, plating, plastics, etc. (ATSDR, 1999). Cadmium (Cd) causes kidney problem, a dysfunction caused by a reduction of glomerular filtrate. Lead (Pb) causes mental disorders in children who may develop problems with memory, learning, and concentration. Pb may also cause anemia because it inhibits the formation of hemoglobin. Chronic exposure to mercury even in small quantities in drinking water may cause psychological and neurological symptoms like tremor, restlessness, anxiety, stress, and depression. Antimony is emitted into the environment mostly as a result of coal burning or with fly ash during the melting of antimony-containing ore (Nriagu & Pacyna, 1988). Oral exposure to high levels of antimony(III) has been associated with optic nerves destruction, retinal breeding, uveitides and could trigger premature birth (Stemmer, 1976). Presence and quantity of these metals were determined in the Nairobi River because even though people may not be drinking water from the river, the water is used mainly for small-scale irrigation projects and the produce is sold to unsuspecting city residents. There are three primary pathways through which humans are exposed to heavy metals: direct ingestion, inhalation, and through skin contact. Ingestion and skin contact exposures are prevalent for elements that are dissolved in water. Children are at a higher risk from exposure to heavy metals than adults because they have a higher rate of cell division (Saha et al., 2016). A study done along the Nile delta showed a disproportionate distribution of heavy metals, i.e., As, Pb, Cd, and Hg with respect to season, geographical area and sampling points in the Nile Delta, Egypt (El-Kowrany et al., 2016). The severe intensity of all these metals is present in all seasons in the source water sampling points of Nile River. There is often a significant decline in

the concentration of most metals with increasing distance from the point of introduction. However, some elements have constant values even over great distances, for instance As and Mn (Saha et al., 2016). This has been explained as a result of natural sources rather than anthropogenic introduction (Saha et al., 2016). The general considered range of carcinogenic risks for As when ingested or in contact with the human skin is10^{-6} to 10^{-4} mg/Kg (ppm) by USEPA (2012) standards.

Freshwater contamination by trace metals in the developing countries has become a major environmental concern (Goher et al., 2014a). Anthropogenic inputs of pollution are rapid and intense, as opposed to natural contamination which is gradual and slow through weathering and leaching (El-Bouraie et al., 2010). Many trace elements above normal are produced by industries, domestic wastes, storm-water from urban areas, landfills and agricultural chemicals (Hashim et al., 2011). Most inorganic pollutants are of significant environmental concern because they are usually non-biodegradable, have a long biological half-life and toxic to plants and animals (Goher et al., 2014b; Singare et al., 2012). Some trace metal contaminants are very toxic even in small concentrations and could lead to bio-accumulation when absorbed over a long time causing damages to the nervous system and other internal organs like the liver and kidneys (Lohani et al., 2008). Different countries have set long-term trigger values (LTV) and short-term trigger values (STV) for heavy metals in irrigation water. These values refer to the maximum and minimum acceptable contamination of water used to irrigate human food (Anzecc, 2000). World Health Organization (WHO, 2006) and USEPA (2012) developed standards for acceptable limits for heavy metals in water used for humans' consumption.

The chemical index of alteration (CIA) is a calculation based on geochemical analysis that has been applied for decades to study the history of silicate minerals weathering into clays (Roddaz et al., 2006). CIA in sediments reflects chemical weathering history of the source of the sediments

(Potter P.E. et al., 2005). It is a quantitative indicator for determining silicate weathering and is defined as $Al_2O_3/(Al_2O_3+CaO^*+Na_2O+K_2O)$ x100%. CaO* is the amount of CaO in silicate fraction and does not include CaO combined with phosphates and carbonates minerals, such as may occur in soil carbonates or biogenic material (e.g. gastropod shells). To avoid potential complications caused by pedogenic and biogenic carbonates, if CaO content is less than that of Na_2O, then the value of CaO is used in computing CIA. If the content of CaO is higher than that of Na_2O, then the value of Na_2O is used in the equation instead of that of CaO. CIA reflects the degree of aluminum silicate minerals, especially feldspar weathering into clay minerals (Fedo et al., 1995). Higher CIA values indicate more chemical weathering and leaching of Na, K and Ca bound minerals (Nesbitt, 1989). The degree of weathering is correlated to the denudation rate of the watershed (Li et al., 2010). Li et al. (2010) further established that the degree of weathering is also affected by average annual temperatures, latitude and the thickness of the soils layer. Weathering activities are also affected by climate and runoff in latitudinal catchments while the underlying bedrock and other factors are secondary (Shao J.Q, et al., 2012, Yang S.Y., et al. 2004). River broadening and floodplains may cause enhanced values of CIA because of weathering of floodplain sediments (Heller P.L. et al., 2001).

1.1.3 The Nairobi River Watershed

The Nairobi River flows through Nairobi City, the capital of Kenya (Figure 1) and is an important resource in the watershed. The river originates from the Ondiri Swamp catchment (Figure 2), about 10 miles to the Northwest. The effect of urbanization is evident from a gradual change of the physical appearance of the flowing water down the gradient and through the city. It is joined by other tributaries along the gradient to form one big channel, the Nairobi River and eventually

merges with the Athi River to the south of Nairobi and flow through the Eastern Province of Kenya and into the Indian Ocean.

Most of the piped water (94%) consumed in Nairobi comes from the Aberdare Ranges to the North of the city while the remaining 6% comes from Kikuyu spring and Ruiru Dam. Nairobi City residents who do not have piped water rely on water vendors who charge them expensively for water, unlike those privileged to have piped water from the County Government. It is estimated that only 10% to 48% of the city residents are connected to the sewage line (Athi Water Services Board, 2011). Two water treatment plants treat industrial and domestic wastes with a capacity of 112,000m^3/day. One of the plants contains stabilization units with the most intensive pond systems in Africa, but only half the capacity has been in use (EACF, 2008). The effluent from these plants is drained into the Nairobi River (NCWSC, 2011). Different groups and institutions have tried to remediate the pollution of Nairobi River in the past, and one important body is Nairobi River Basin Rehabilitation Program (NRBP). NRBP was created to bring together the government of Kenya, development partners, private sector and civil societies to spearhead the management of the rivers in the basin (African Development Bank, 2010). They determined the sources of pollution into the rivers as coming from uncollected garbage, human wastes from informal settlements, industrial wastes in the form of gaseous emissions, liquid effluents, agrochemicals, petrochemicals, metals and overflowing sewers. A ten-points strategic plan was proposed to curb the proliferation of pollution and they include stoppage of illegal discharge and development and implementation of the integrated solid waste management system. Moreover, the benefits of rehabilitating and maintaining the rivers' system were enumerated, and they included provision of safe and clean water, ecosystem services, economic improvement, employment, recreational, tourism, security, accessibility, and a clean environment for Nairobi residents (Ministry of Environment and Mineral

Resources, Kenya, 2009). However, garbage and other human effluent along the banks of the rivers' channels are still a problem, and the water quality is still unpleasant by physical appearance.

1.2 Goal and Objectives

The main goal of this study was to compare the relationship between LULC within Nairobi River Watershed with the quality of water in Nairobi River.

Objectives

i. To establish the extent of LULC change in the watershed for the past three decades (between May 1986 and May 2015).

ii. To determine the rate of urbanization leading to the creation of impervious surfaces in the watershed

iii. To delineate the Nairobi River watershed and determine the current proportions of LULC.

iv. To determine the concentrations of inorganic elements and mineralogy of the Nairobi River channel's sediments.

v. To establish the relationship between the concentrations of inorganic elements, LULC, and the distance from the origin of Nairobi River.

1.3 Hypotheses

i. There has been a significant change of LULC in Nairobi River Watershed in the past 3 decades.

ii. Development of impervious surfaces (urbanization) in the watershed have increased in the last three decades

iii. There is a significant amount of inorganic pollutants in Nairobi River as a result of anthropogenic activities in the watershed.

iv. The amount of inorganic pollutants increased down the river gradient and it is expected that the urban areas experienced more pollution than other classes.

1.4 Justification of the Study

There is a growing need for the provision of clean water to cater for the demands of the ever-increasing humans' consumption, irrigation and other uses in many parts of the world. These requirements have been increased by contamination of existing water resources in crowded places. The problem is expected to worsen in future because of the projected climate change that is likely to affect the hydrological cycle, while at the same time the population is predicted to increase rapidly especially in cities. It is logical for water managers to take stock and protect all the possible sources of water especially the natural ones. One way of doing this is by trying to remediate the polluted surface water by putting in place measures that will alleviate the menace of water pollution and prevent future surface and groundwater contamination. To achieve this, toxicological analyses of hydrological resources is necessary. Determination of the types and intensity of contaminants in water assets, the establishment of possible sources of pollution and proposals for practical ways in which rivers can be managed from pollution is paramount. This study determined the type and sources of primary inorganic pollutants of concern in Nairobi River, an important river flowing within the heart of Nairobi, the capital city of Kenya. It also sets a base upon which city planners and water managers in Nairobi could apply measures that will address pollution concerns in Nairobi Rivers. Moreover, there is hardly any published study that has been carried-out in NRW, focusing on the LULC change and the effect of LULC on water quality.

2 METHODS

2.1 Study Area

2.1.1 Water Resources

The study was conducted in the Nairobi River, the main river flowing through Nairobi City, Kenya. The River originates from Ondiri Swamp located about 10 miles northwest of the city, and the swamp has an area of about 32ha. It is joined by other rivers and tributaries at different points within the city before merging with the bigger Athi River to the south of Nairobi. Other rivers and tributaries join the Nairobi River down the gradient, i.e., the Ruiru, Kamiti, Kasarani, Ruaka, Karura, Gitathuru, Kirichwa, Motoine-Ngong, and Mathare Rivers. The rivers draining the watershed are perennial, and there is a good aquifer between the Kerichwa Tuffs and the underlying Nairobi phonolite (Figure 1 and 4). However, the fluoride content of the aquifer tends to be high (Saggerson, 1991). Nairobi City got its name from the Nairobi River which is a Maasai (a tribe in Kenya and Tanzania) translation for cool water. The City is located at 1°09′S 36°39′E and 1°27′S 37°06′E, while its administrative boundaries encompasses a total area of 696 Km2 (269 sq mi).

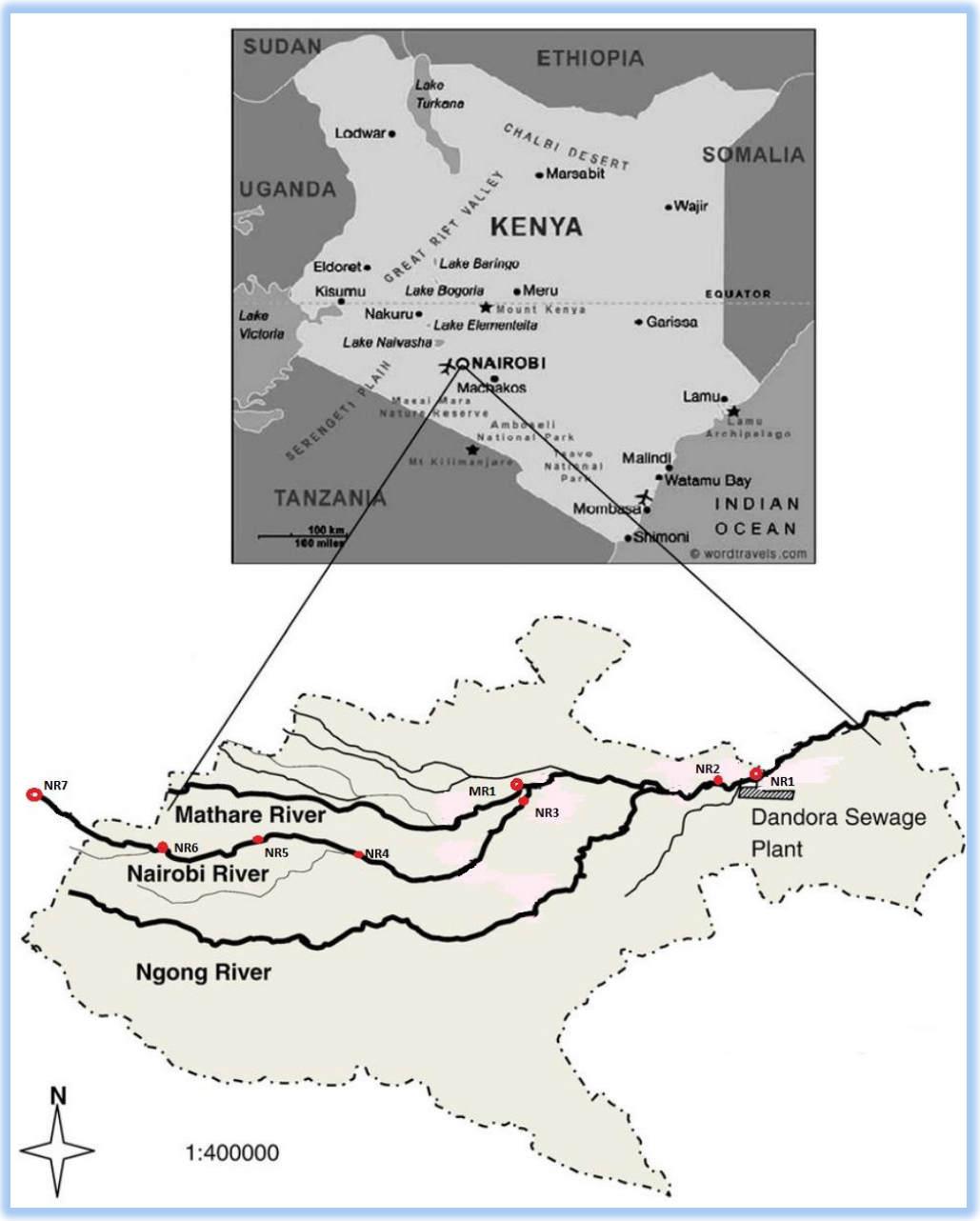

Figure 1 Nairobi City political boundaries and Rivers

The map shows political boundaries of Nairobi City, the main rivers and tributaries and the red marks are the approximate location where samples for analysis were recovered (Source: http://www.google.com)

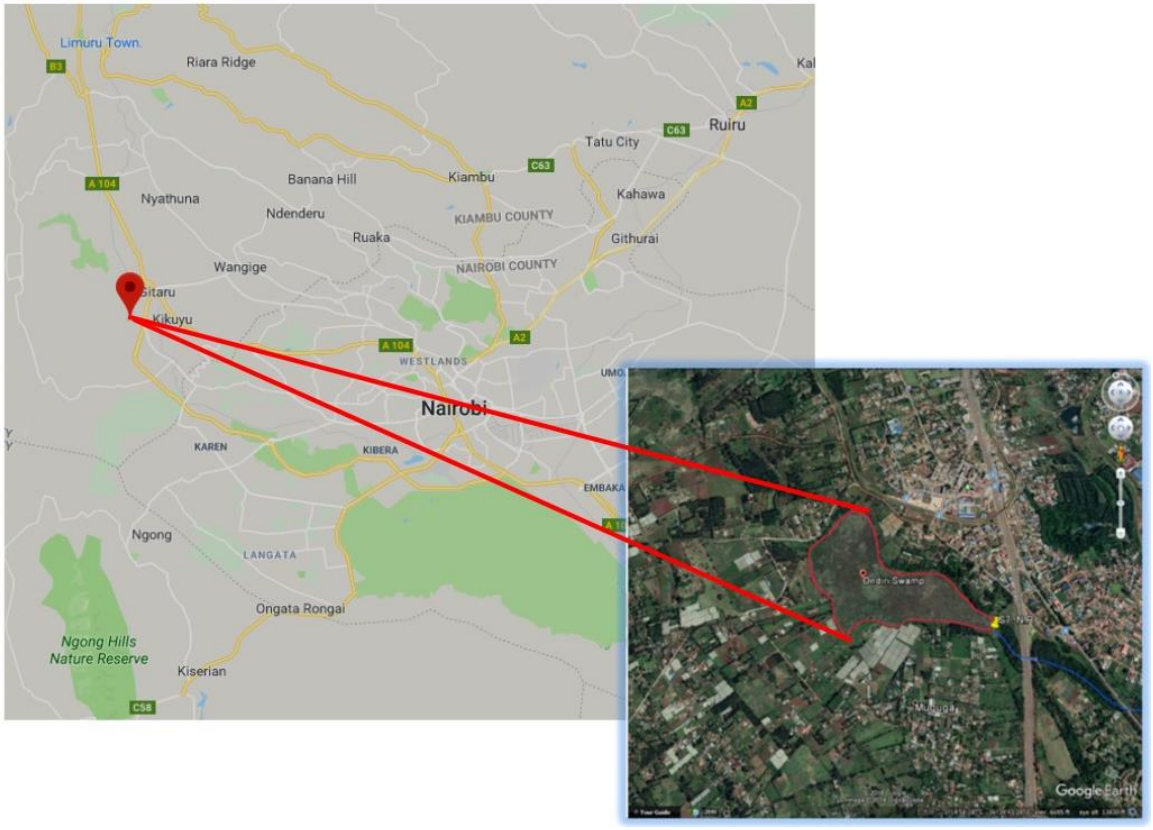

Figure 2 Ondiri Swamp

These are extracts from Google map showing the location of Ondiri Swamp, the origin of the main channel of Nairobi River (Google Earth)

The rivers' and tributaries' within the city have been significantly encroached and abused, with massive amount of solid wastes along the banks (Figure 3). Industrial wastes and domestic sewage disposals are a big problem. In September 2016, the County government of Nairobi mapped 278 polluters mainly factories in Nairobi industrial area. During the same time, there was a mop-up campaign against residential houses that were not connected to the main sewage system and several property owners that were found draining untreated wastes into the river were apprehended (Daily Nation, Kenya, 2016). Those washing vehicles along the rivers were ordered to acquire water recycling machines that could separate soaps and mud from water or otherwise their permits would be revoked. According to a local daily news article, there are definite steps

towards cleaning Nairobi River, but a lot more is required if the quality of water in the river is expected to improve for safe human consumption.

Figure 3 Solid waste along Nairobi River

These are images captured along Nairobi River channel in the urban class and they show the extent of solid waste contamination along the river. Plastic bags are a menace all along the river especially in the urban area.

2.1.2 Geology of Nairobi River Watershed, Kenya

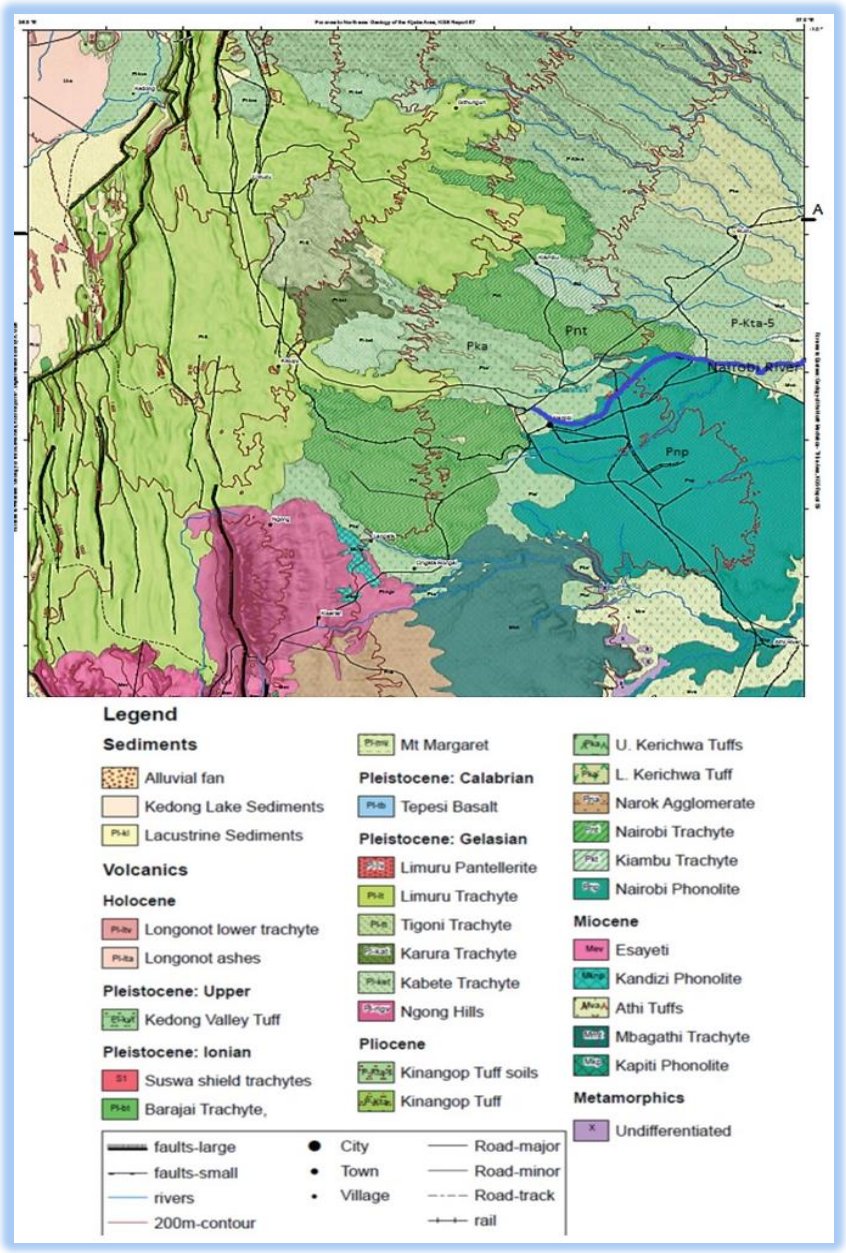

Figure 4 Geology of Nairobi River Watershed

A geological survey map and legend of Nairobi River Watershed (Guth and Wood, 2013), Nairobi River is marked with a blue line. The northern side of Nairobi River is dominated by Nairobi trachyte (Pnt), Kerichwa tuff (Pka) and Kinangop tuff (P-Kta-5). The southern part is mainly the Nairobi phonolite (Pnp)

The volcanic materials dominating the watershed are mainly phonolite, trachyte, and tuff dating to Pliocene. The Northern and the Western regions are predominantly occupied by Kerichwa tuff (Pka), Nairobi trachyte (Pnt) and Kinangop tuff (P-Kta-5) (Figure 4). The southern part is mostly occupied by Nairobi phonolite (Pnp). Kerichwa and Kinangop tuffs date to about 3.34 to 3.70 ma., they are trachytic tuffs and are often welded and overlie the Nairobi trachyte (Baker et al., 1988). There is a likelihood of bleaching and clay alterations which most likely represents the weathering situation before the eruption of Limuru trachytes. Nairobi trachyte dates to about 3.17 to 3.45 ma., and it is greenish and sometimes has tabular feldspar phenocrysts. Nairobi Phonolite is the oldest of the Pliocene series, dating 5.20 ma. It is a black to blue material that erupted as a number of flows. Lava is vesicular in the upper flow section but rarely contain amygdule. These phonolites are easily distinguished from the Kapiti Phonolite because they lack substantial phenocrysts (Saggerson, 1991).

2.1.3 Soil

The Nairobi River originates in an area with a deep red soil with high fertility, probably nitisol and andosol soils (Figure 5). The city lies within a well-drained reddish soil in the north to poorly drained, dark and moderately deep to deep vertisol to the south (Sombroek and Pauw van der, 1980). Vertisols are soils with high proportions of expansive clay known as montmorillonite that forms deep cracks under dry conditions. Vertisols have a deep A horizon but no B horizon (Donovan, 1981). Nitisols are deep red soils with clay content of more than 30% and are found in the tropics and subtropics. Nitisol support tropical rain forests and savannah vegetation but are frequently low in phosphorous and base status (Delvaux and Brahy, 2014).

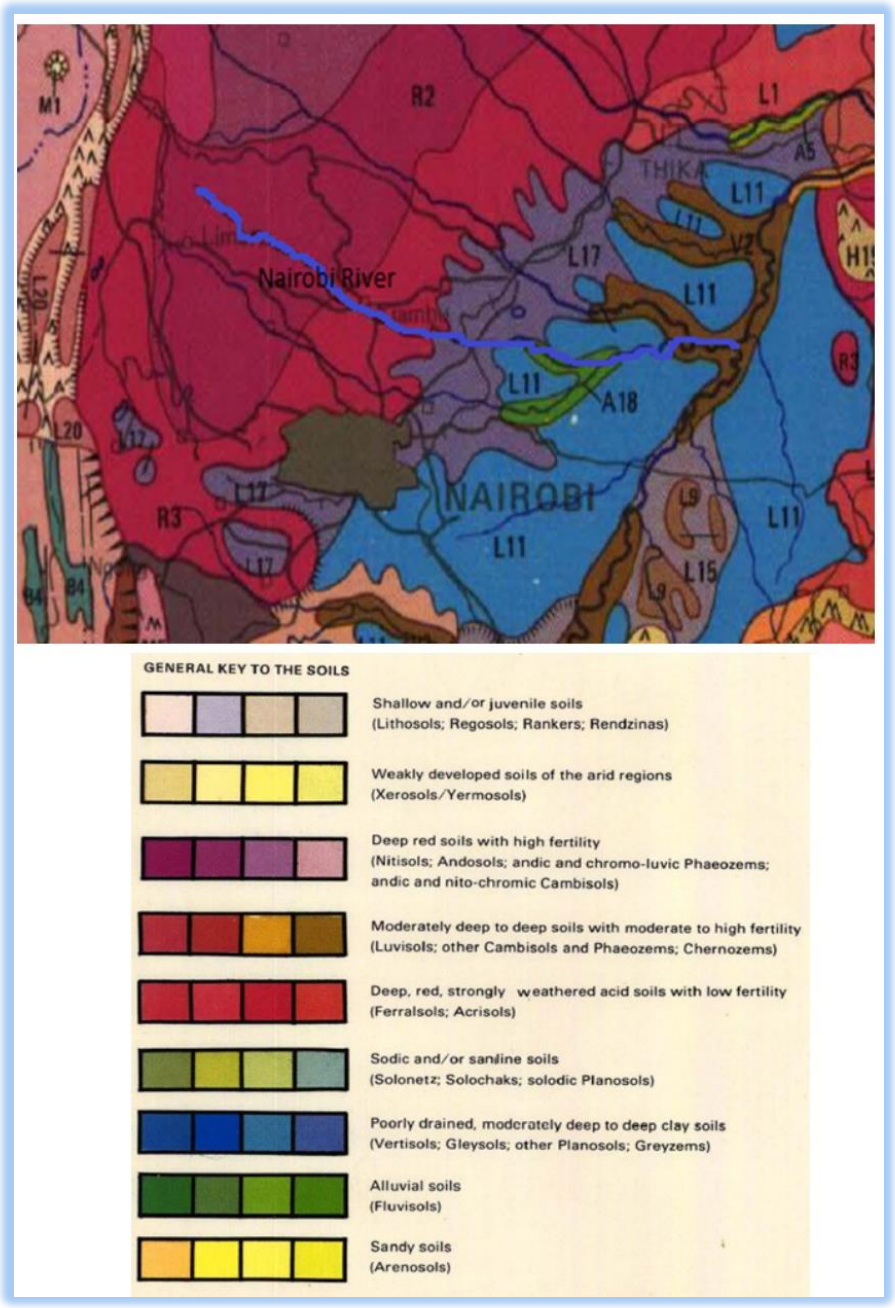

Figure 5 Soil survey map

A soil survey map and legend of Nairobi area (Adopted from Sombroek and Pauw van der, 1980). Nairobi River originates from a more reddish and well drained soils in the northwestern side of NRW to a poorly drained and dark soils in the southeastern side.

2.1.4 Climate

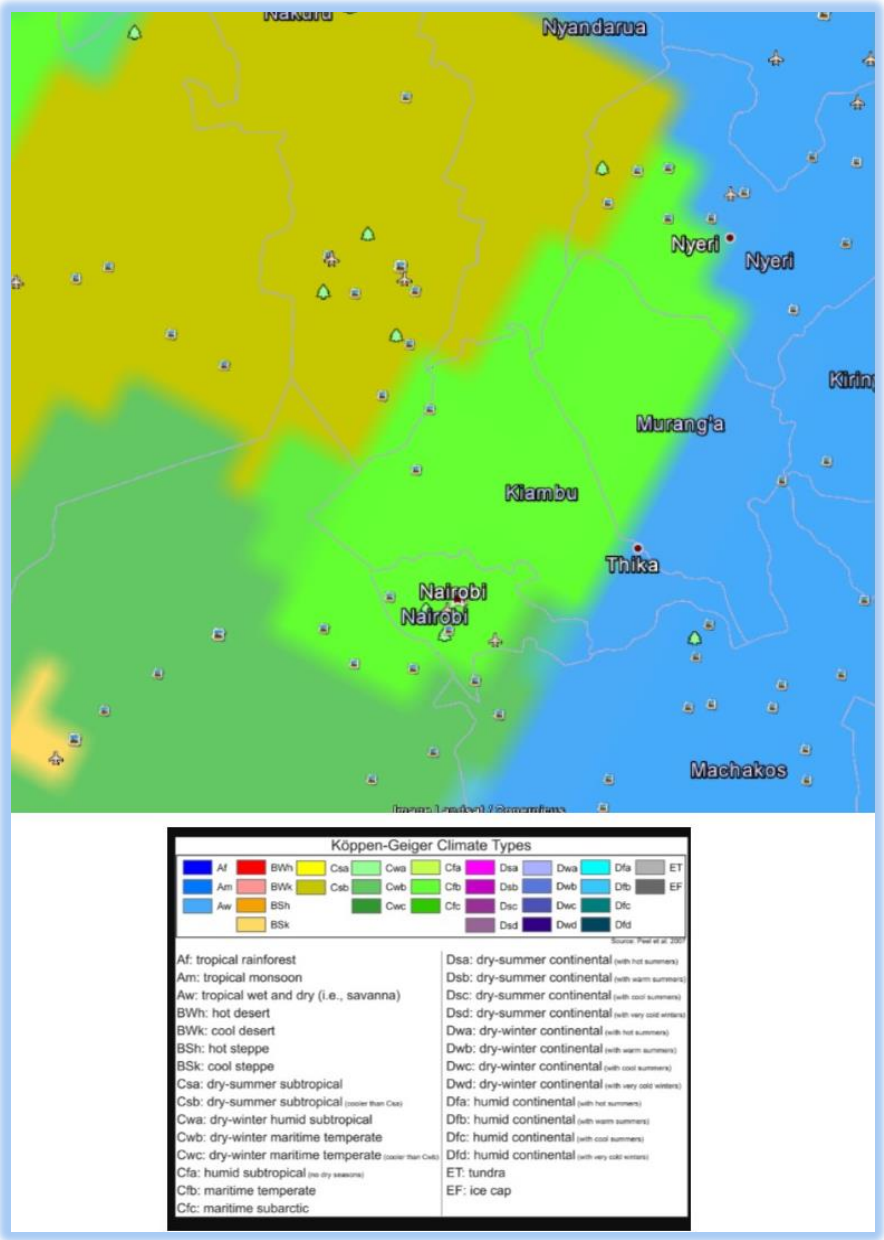

Figure 6 Köppen-Geiger Climate Type

The Climate type of NRW is largely humid Sub-tropical but in the western side there is a significant portion dominated by Tropical wet and dry (Savannah) climate.

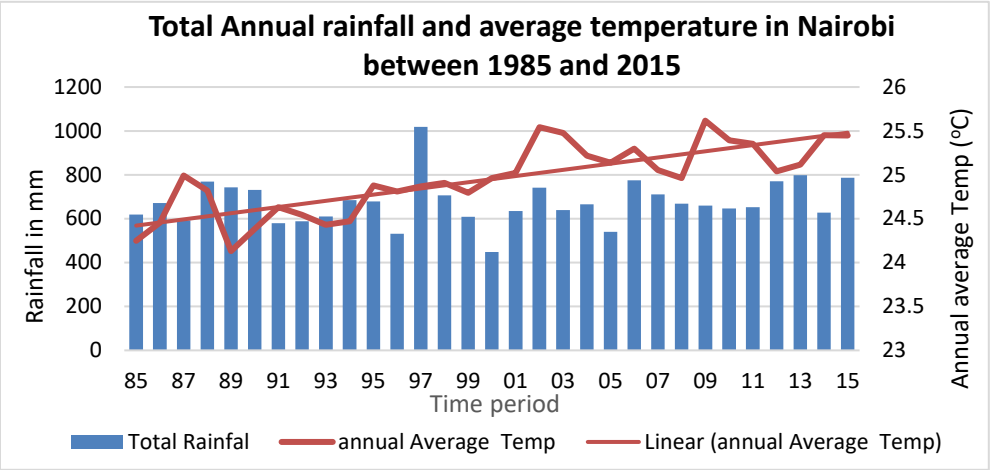

Figure 7 Total annual rainfall and average temperature from 1985 to 2015

The data was retrieved from the World Bank Group, Climate Change Knowledge Portal for Development Practitioners and Policy Makers

The larger part of Nairobi area has a humid sub-tropical climate (Cfa) type according to Köppen-Geiger Climate characterization. The western region of the watershed is dominated by the tropical wet and dry (Savanah) climate (*Figure 6*). The average annual precipitation remained very constant in the last three decades except in the year 1997 when the total annual rainfall (1018 mm) was higher because of El Niño -Southern Oscillation (ENSO) phenomenon (*Figure 7*). The lowest annual precipitation of 448 mm was recorded in the year 2000 because of a prolonged drought. The average annual temperature has, however, increased by about 1°C during this period, i.e., from 24.5°C to 25.5°C.

2.2 Land-Use and Land-cover

Remote sensing and Geographic information system techniques were used to delineate the Nairobi River Watershed and to classify LULC pattern. Multispectral Landsat digital images were acquired from the United State Geological Survey (USGS) visualization viewer, GLOVIS (http://glovis.usgs.gov) website and analyzed using ERDAS-ERDAS IMAGINE and ArcGIS

software for RS and GIS respectively. Both images were captured from Landsat satellites, one from May, 1st 1986 and the other one from May, 1st 2015. The 1986 image is a Landsat 5 TM (Thematic Mapper) while the 2015 image is a Landsat 8 OLI (Operational Land Imager), both with a spatial resolution of 30 m for the main bands. Image rectification and atmospheric corrections were performed on both images to improve the accuracy of the results. Delineation of the watershed's boundary was done using ArcGIS on a SRTM (Shuttle Radar Topography Mission) digital elevation model (DEM) data of 90m resolution, obtained from USGS. Watershed delineation processes from ArcGIS involved the filling of sinks in the DEM, flow direction and accumulation, streams' network and links and finally the area-wide drainage basin from a pour point. All the stream orders draining water to Nairobi River were included in the watershed. The watershed boundary layer was used to extract the study area from the Landsat images and then used for further analysis. The two image extracts were classified using the unsupervised classification method in ERDAS Imagine, whereby 20 iterations were set to determine 36 spectral classes. From these spectral classes, five informational classes, i.e., water, forest, agriculture, bare-ground, and urban were established, and the results from both images compared to detect the change in LULC in the watershed from 1986 to 2015.

2.3 Geochemistry

The geochemistry of Nairobi River was based on sediment samples collected along the river channel. Eight samples were selected randomly along the river and georeferenced. Two samples (NR7 and NR6) were obtained from a more agricultural section of the watershed and less developed. Four samples (NR5, NR4, NR3, and MR1) were collected from an increasingly developed section. Sample MR1 was not picked from Nairobi River but from Mathare River, a tributary that joins NR close to the point where this sample was collected. It is noteworthy that

sample MR1 was picked near sample NR3 because they both represent the urban class in this analysis. Sample NR2 was collected from a less developed part of Nairobi where urbanization is currently spreading to. The last sample (NR1) came from adjacent the biggest sewage treatment plant in Kenya and East Africa. This sample was meant to test the effects of the return flow from the sewer treatment plant.

Analysis of inorganic elements was conducted on each sample, provided by the commercial analytical company ALS Global (Reno, Nevada). Oxides of major elements were analyzed using inductively coupled plasma (ICP) method coupled with Atomic emission spectrometry (AES). In this analysis, samples were decomposed using lithium metaborate ($LiBO_2$) or lithium tetraborate ($Li_2B_4O_2$) fusion. The concentration was calculated from the determined elemental concentration. The compounds analyzed using this method were oxides of aluminum (Al_2O_3), barium (BaO), calcium (CaO), chromium (Cr_2O_3), iron (Fe_2O_3), and magnesium (MgO). Others included manganese (MnO), phosphorous (P_2O_5), potassium (K_2O), silicon (SiO_4), sodium (Na_2O), strontium (SrO), and titanium (TiO_2). Inorganic sulfur and carbon were analyzed using LECO technology which is a combustive technique for analyzing metals and alloys for sulfur, carbon and some other elements. LECO analysis detects levels as low as 0.01% of both sulfur and carbon in a sample. Base metals were analyzed using MS82 which is a four acid digestion technique for analyzing ultra-trace levels. In this method, samples are decomposed using Lithium Metaborate fusion and analyzed by Inductively Coupled Plasma – Mass Spectroscopy (ICP-MS). Volatile trace elements were digested using aqua regia digestion and analyzed using ICP-MS. Major elements oxides were recorded as percentages while trace elements were reported in parts per million (ppm).

2.4 Mineralogy

Each sample was analyzed at Georgia State University using X-Pert PRO PANalytical X-Ray diffractometer equipment running from 0.5^{o} to 45^{o} for clay (oriented slides') samples and 65^{o} for powdered samples, and the generator set at 45kV tension and 40mA current. This analysis was to determine the mineral composition of the sediments. Determination of mineral composition was vital because it explained whether the geochemistry of the channel sediments was as a result of mineral precipitation or from anthropogenic activities. Soil fractions were separated using particles settlement technique adopted from Jackson et al. (1950). This technique allowed sorting out of four sediments fractions which included sand (> 50 microns), coarse silt (20 – 50 microns), fine silt (2 -20 microns) and clay (< 2 microns). The procedure involved suspending the sediment in distilled water and waiting for a specific duration of time before decanting. 2% sodium chloride solution was added to bring the solution to a weaker base (about pH 9.5) to facilitate flocculation. For larger particles of sand (>50 microns) settlement was timed for 40 seconds for every 4 inches (10 cm) column height of the suspension, after all the particles had been suspended. The supernatants were re-suspended, allowed to settle for 40 seconds per 4 inches' column height of the suspension and then decanted. Re-suspension and decanting were repeated several times until all the clay and silt were separated from the sand. The >50 microns fractions were then dried at 50^{o}C and ground to a finer powder for bulk minerals analysis with XRD.

After all the sand was extracted, the suspension was then stirred thoroughly for about 30 seconds until all the particles were well mixed in the suspension. Silt settlement was timed at 5 minutes for every 4 inches' column height of suspension. After five minutes, the suspension was carefully decanted, and the supernatant re-suspended in distilled water for 5 minutes for every 4 inches' column height, after which the suspension was decanted. This process was repeated several

times until all the clays were removed, which was marked by attaining similar results after consecutive cycles. This process removed all the particles within the range of 20 – 50 microns, which were then dried at 50^{o}C and ground into a fine powder. The larger grains (2-20 microns) in the suspension were removed by letting the suspension settle for eight hours of every 4 inches column height of the mixture, after which it was decanted. Petrographic Microscope slides were prepared with the 2-20 microns supernatant and the rest dried at 50^{o}C and then ground to a fine powder for bulk minerals analysis with XRD.

Separation of < 2 microns fraction with the rest of the suspension was done by adding a few drops of calcium carbonate solution to the mixture. Calcium carbonate hastens flocculation, whereby all the particles settle after a couple of minutes, leaving behind a clear liquid. The clear liquid was carefully decanted and the sediments re-suspended in distilled water and centrifuged for eight minutes at 1100 rpm. The clear liquid was decanted and the samples suspended again in distilled water and centrifuged. This process was repeated for a couple of times to wash the samples off the calcium carbonate. Caution was, however, exercised to avoid resuspension of clay particles into the distilled water when all the calcium carbonate was rinsed from the sediment. The supernatants were used to prepared glass slides for clay minerals' analysis using the X-Ray Diffractometer. Two slides were prepared from each sample whereby each slide was done by adding about 20cc of well-mixed clay and distilled water. The rest of the clay sediments were left in the suspension. Mineralogy studies were conducted on powdered samples, i.e., sand (>50 microns), silt (20-50 microns) and finer particles (2-20 microns); and slides, i.e., clay (<2 microns).

The powdered fractions were analyzed for bulk analysis using PW 3064 sample stage which is the most convenient for powdered samples. Clay samples on petrographic microscope slides were examined using PW 3071 sample stage which is the most appropriate for clay samples.

Four XRD patterns were conducted on clay samples to determine the clay mineralogy of Nairobi River channel's sediments. The following treatments were performed to determine the clay mineralogy of NR.

1. Samples were air dried for about 24 hours before analysis with the XRD.
2. The air-dried samples were heated at about 550^{o}C for one hour before the analysis with the XRD.
3. Air-dried samples were treated with ethylene glycol for 24 hours. This was to expand the swelling clay and mixed layered clays to aid in identification.
4. Air-dried samples were lastly treated with formamide to determine whether there was halloysite in the kaolinite group, in line with Churchman et al. (1984). This was done by spraying the air-dried slides with formamide and analyzing them within 20 to 30 minutes after the application.

2.5 Loss-on-ignition Analysis

The commercial geochemical analysis provided a total LOI measurement at 1000^{o}C. In additional to this, I carried out stepwise loss-on-ignition analysis to provide more detailed data. Each sample was analyzed for carbonates and inorganics using the loss on ignition (LOI) technique. For each sample, three measurements were analyzed and the average results recorded to reduce errors. The crucibles used for analysis were weighed before and after samples were added and heated in a closed furnace at 100^{o} C temperature for over 12 hours to extract all the water. The samples were then allowed to cool and measured again to determine the weight of water after which they were reheated at 550^{o} C temperature for four hours. Heating the samples at 550^{o} C removed all the volatile organic matters which were determined by measuring the weight of the remaining residue. Lastly, the samples were heated at 1000^{o}C temperature for 2 hours and the final

weight measured after cooling. This process allowed the determination of the organics and carbonates in the samples.

2.6 Statistical Analysis and Data presentation

The data were analyzed using descriptive statistics, Pearson's correlation coefficient (r) to compare the concentration of heavy metals down the river gradient. Results were presented in summary tables, graphs, and histograms.

3 RESULTS

3.1 Nairobi River Watershed Delineation

The ArcGIS hydrology toolset was used to delineate the watershed from an SRTM digital elevation model of 90 meters resolution ((Figure 8). The image was acquired from the USGS website. The watershed covers the total land area (187,500 Ha) that contributes flow to the pour point marked on the figure, just before Nairobi River connects to the Athi River. It mainly lies within Kiambu County (141,400 Ha), Nairobi City (45,300 Ha), Nyandarua County (623 ha) and a very small portion in Machakos County (195 Ha). Figure 8 also shows the streams' network within the watershed and those of the neighboring drainage basins. The watershed output image was converted into a shapefile in ArcGIS conversion tools and used to mask the area of interest from the landsat images (Figure 10) in ERDAS Imagine software.

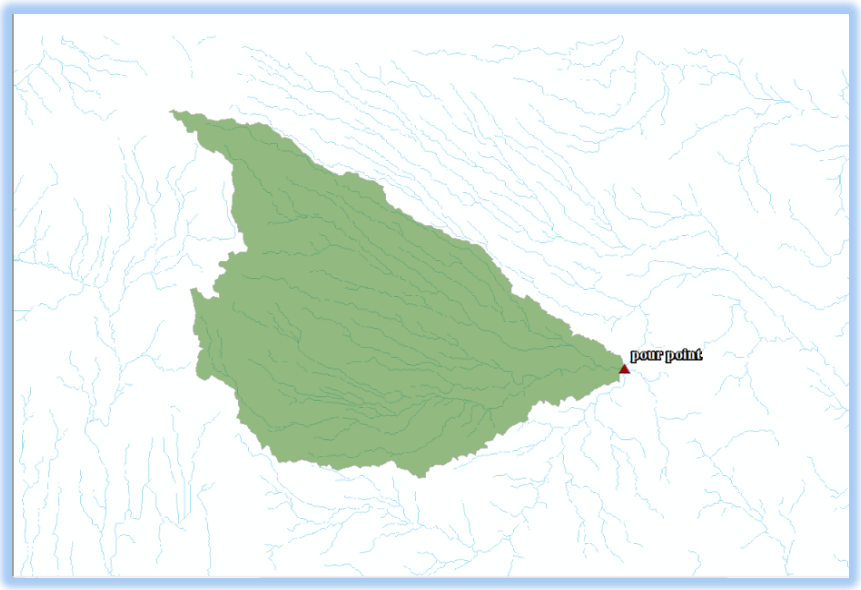

Figure 8 Nairobi River Watershed

3.2 Land-Use and Land-cover

3.2.1 Multispectral Landsat Images

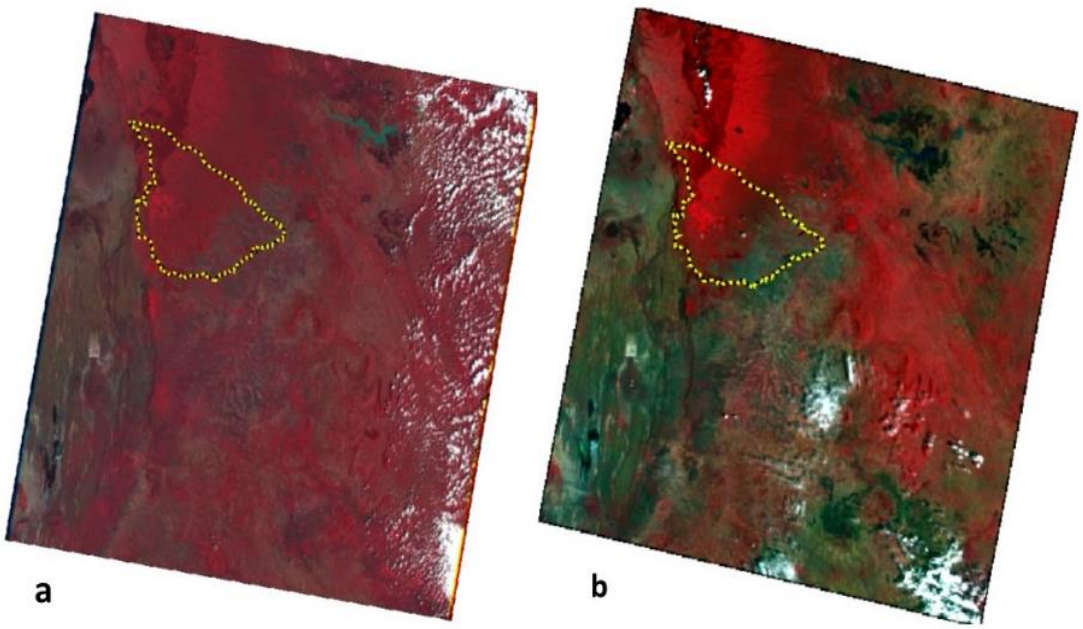

Figure 9 Multispectral Landsat images used in the study

a, Landsat 5 TM Image taken on 05/01/1986 and b, Landsat 8 OLI image taken on 05/01/2015, both displayed in false color infrared scheme and showing the spatial location of NR Watershed (bands 4, 3, 2 for TM and 5, 4, 3 for OLI displayed as red, green, and blue, respectively).

Two digital multispectral Landsat images were downloaded from the USGS website (Figure 9 a, and b,). The images were selected at 0-20% cloud cover tolerance because of lack of better images with lower percentages of cloud cover. The first image is a Landsat5 TM image acquired on May 01, 1986 and the second is a Landsat8 OLI acquired on May 01, 2015. Both images are displayed in a false color infrared scheme where the red, green and blue bands correspond to layers 4,3,2 in Landsat 5 TM and layers 5,4,3 in Landsat 8 OLI.

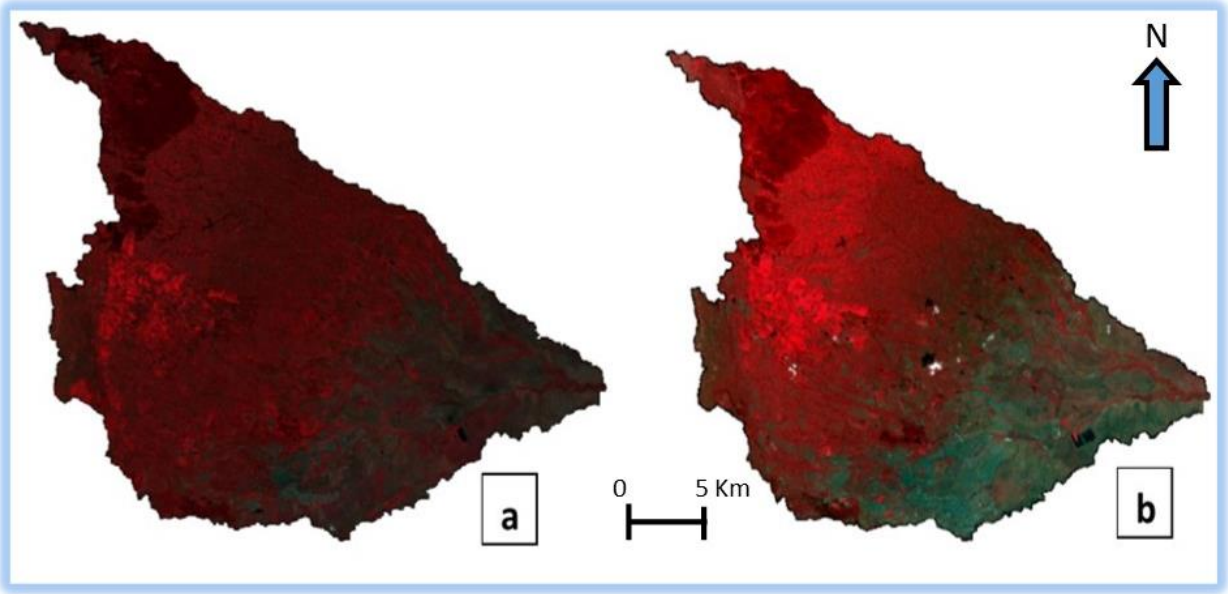

Figure 10 subsets of Landsat images showing the area of interest in false color

a) Landsat 5 TM and b) is a Landsat 8 OLI extracts representing Nairobi River Watershed and displayed in false color infrared (bands 4,3, and 2 for TM and 5,4,3 for OLI displayed as red, green, and blue, respectively).

Nairobi River Watershed area of interested was masked from both Landsat images as displayed in Figure 10 a, and b, above. The extracts are also presented in false color infrared to give vegetation the characteristic reddish appearance for easier identification. Healthy vegetation reflects a lot of the red band in the visible portion of the electromagnetic radiation and therefore

the brighter the red appearance, the healthier the vegetation cover. Urban areas and constructed spaces appear bluish to greyish in this scheme because they reflect less radiation while water appears dark due to its property of absorbing most of the radiation that falls on it.

3.2.2 LULC Change Detection

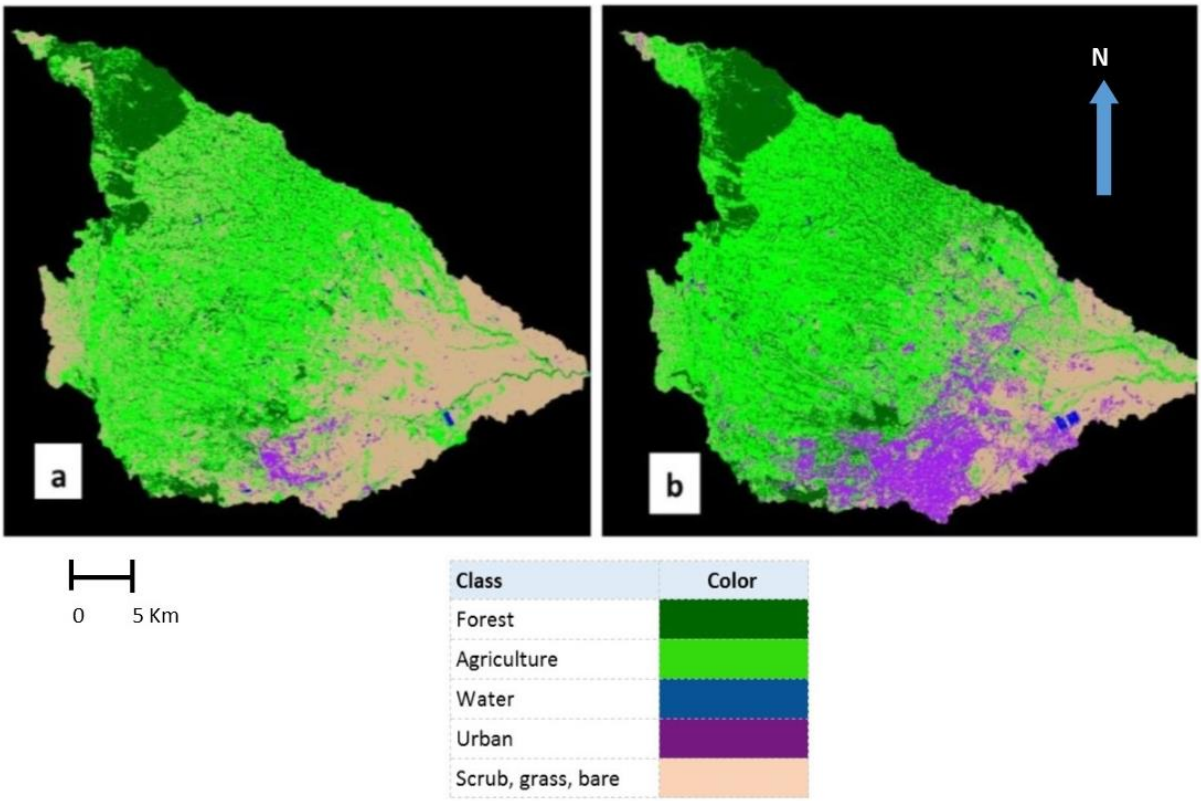

Figure 11 LULC change image

Images a, and b, show the classification of LULC of NRW on 5/1/1986 and 5/1//2015 respectively. The purple color shows urban, dark green shows forest cover, light green is agricultural area, blue is area under water and tan is scrub/grass/bare.

From Figure 11 above and Table 1 below, in 1986, 14% (25,350 ha) of the total land area of NRW was under forest. In the same year, 0.3% (566 ha) was covered by water, 41% (77,745 Ha) was under agriculture, only 3% (4,746 ha) was urban, and 42% (79,120 ha) was scrub/grass/bare. In 2015, forest cover increased to about 17% (32,028 ha) of the total land surface area. Water occupied about 0.4% (785 ha) in the year 2015, agriculture increased cover to 46%

(86,362 ha), urban had 12% (22,243 ha), and the area under scrub/grass/bare shrunk to 25% (45,929 ha).

Table 1 LULC classification of Nairobi River Watershed in 1986 and 2015

LULC	1986 area (Ha)	2015 area (Ha)	% area 1986	% area 2015	Change (Ha)	% Change
Forest	25,349.70	32,028.20	13.52	17.10	6,678.5	26
Agriculture	77,744.60	86,362.50	41.46	46.10	8,617.9	11
Water	566.46	784.64	0.30	0.42	218.18	39
Urban	4,746.00	22,243.30	2.53	11.87	17,497	369
Scrub/grass/bare	79,119.70	45,928.83	42.19	24.52	- 33,190.87	-42

This Table displays the total area in Ha of each LULC in 1986 and 2015 respectively, their percentage cover and the differences between the two periods in Ha and percentages. The percentage change was computed from the change in Ha divided by the specific LULC in 1986.

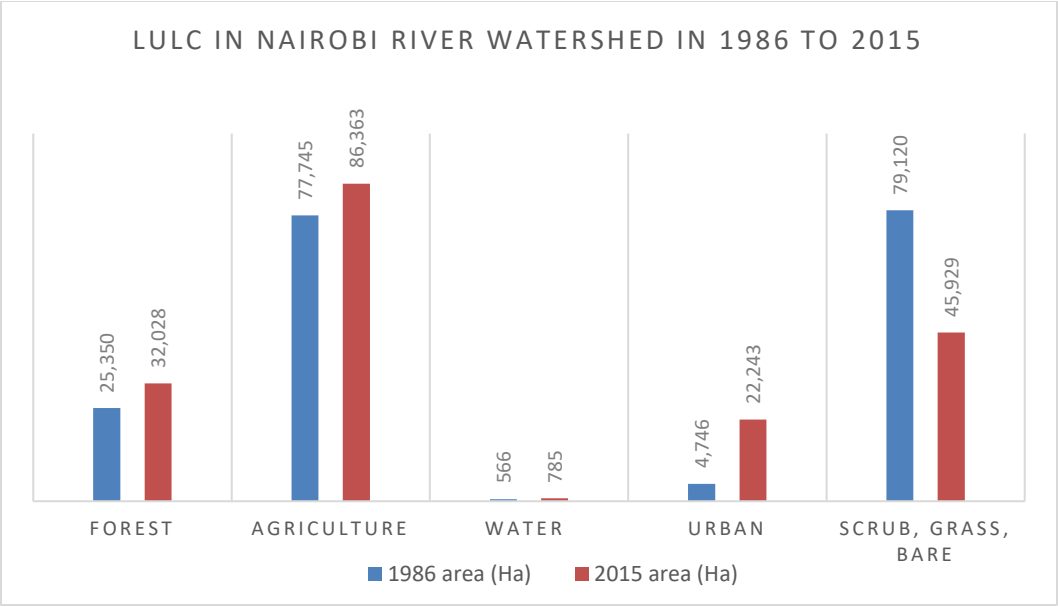

Figure 12 LULC of Nairobi River Watershed in 1986 and 2015

During the 30 years' period, urban development increased by 369% (17,497 ha), and this was the greatest percentage increase of all LULC. Water class increased by about 39% from 566 Ha to 785 ha. Agriculture class gained coverage by about 11% while the area under forest increased by 6%. Scrub/grass/bare decreased coverage the most by about 42%.

3.2.2.1 Urbanization, Deforestation, and Agriculture

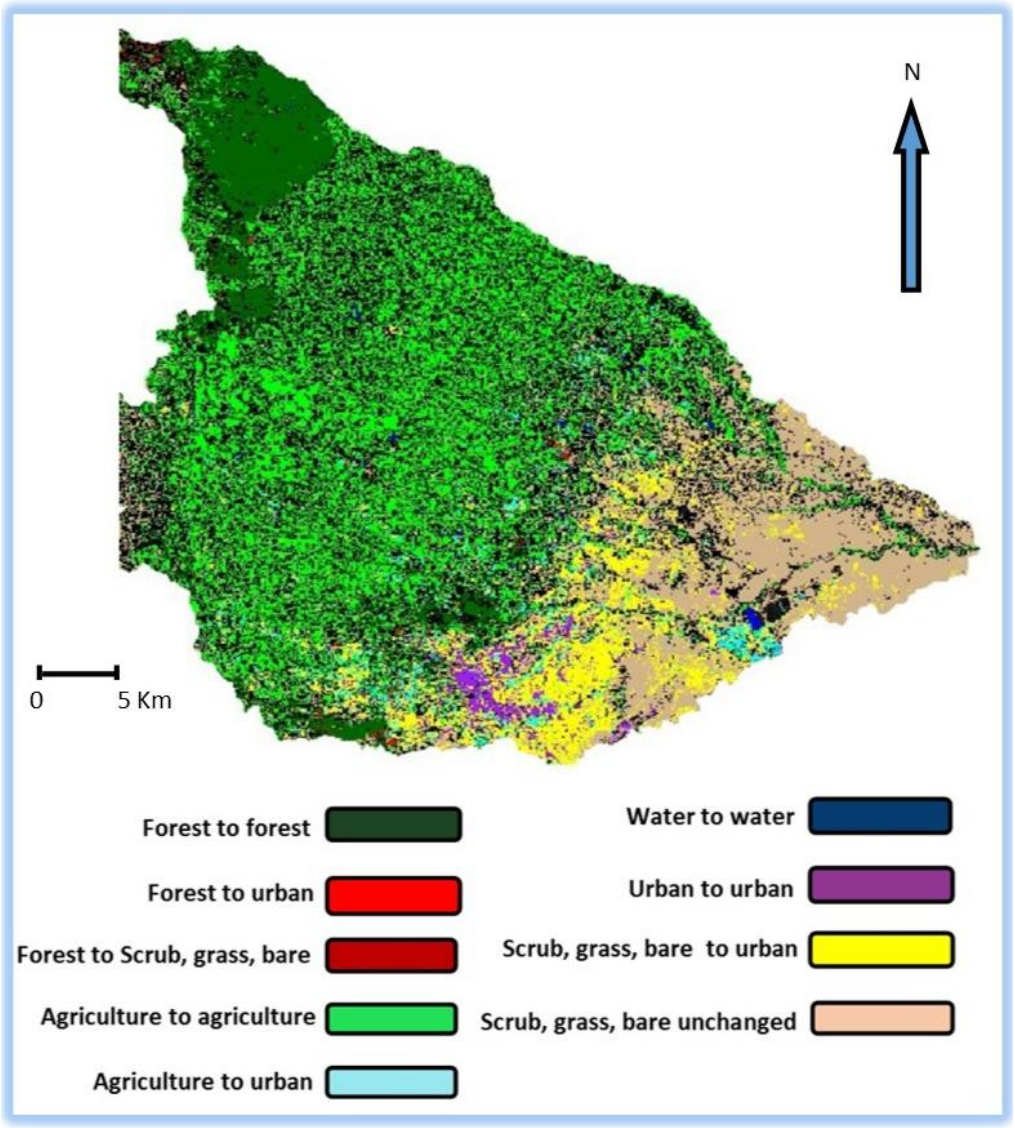

Figure 13 LULC Change, Urbanization and Deforestation

Figure 13 above presents the trend in Urbanization and deforestation between the year 1986 and 2015. The areas marked with red represent forests that were converted into urban while the brown color shows areas that were forest and turned into scrub/grass/bare. Cyan symbolizes areas that were under agriculture and converted into urban areas. Yellow represents scrub/grass/bare land that turned into urban. Figure 14 below highlights the conversion of other LULC classes into agriculture whereby the areas shaded with red are portions of forests that were converted into agriculture. Cyan shows areas that were converted into agriculture from scrub/grass/bare class.

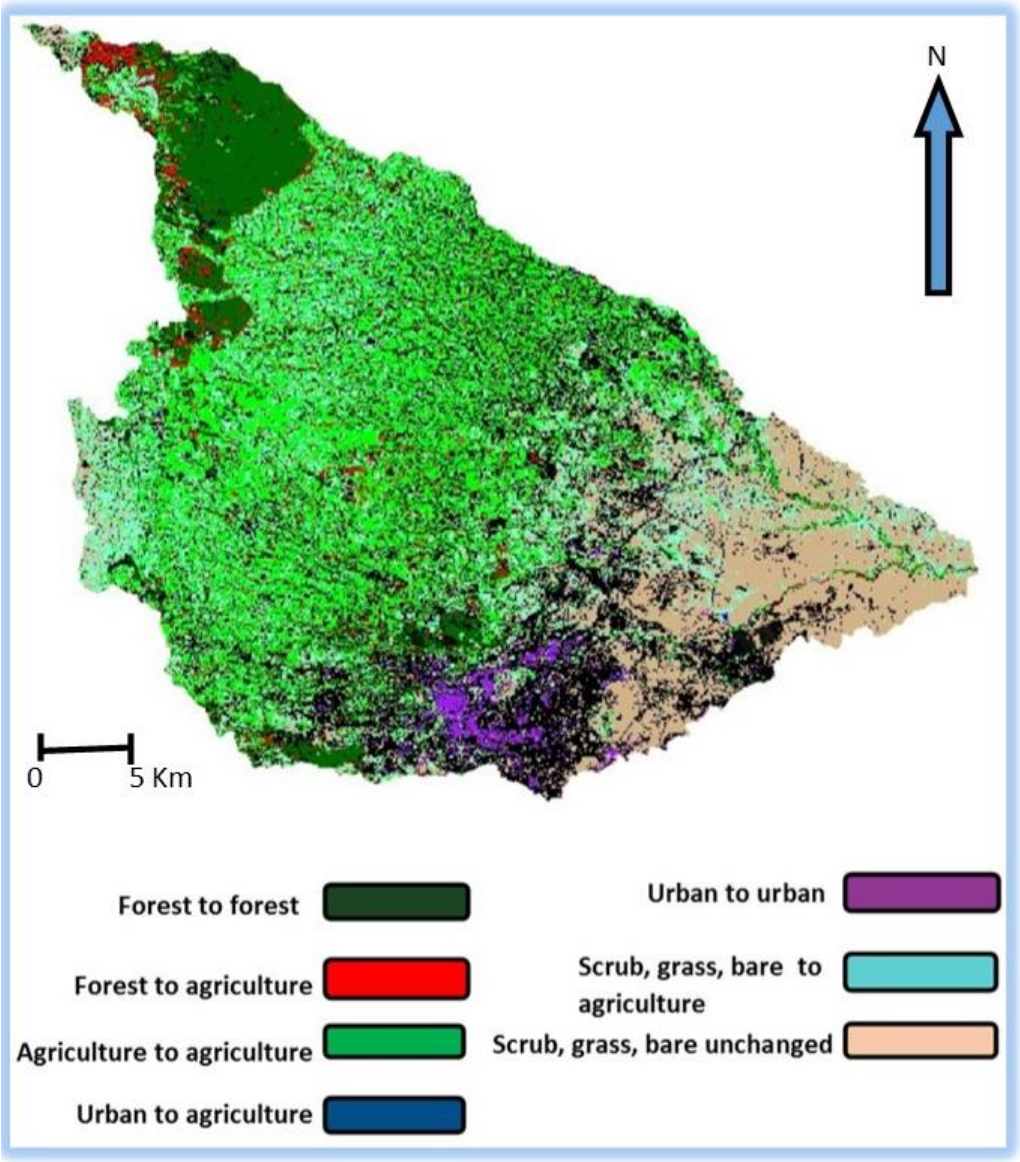

Figure 14 LULC Change, Agriculture and Deforestation

Table 2 and figure 15 show how LULC gained or lost during the study period. The water class gained 423 Ha and lost about 204 Ha between 1986 and 2015. The forest class gained cover by about 14,748 Ha and lost about 8.041 Ha. Agriculture gained about 35,746 Ha and lost about 27,093 Ha during the period under consideration. The urban class had the least loss relative to the gain, whereby the class lost about 1,944 Ha and gained 19,426 Ha. The scrub/grass/bare class gained about 12,682 Ha and lost 45,753 Ha which was the greatest loss for all classes.

Table 2 LULC gains and loses between 1986 and 2015

Class	Gain	Loss	Net Change
Forest	14,748	8,041	6,707
Agriculture	35,746	27,093	8,653
Water	423	204	219
Urban	19,426	1,944	17,482
Scrub/grass/bare	12,682	45,753	-33,071

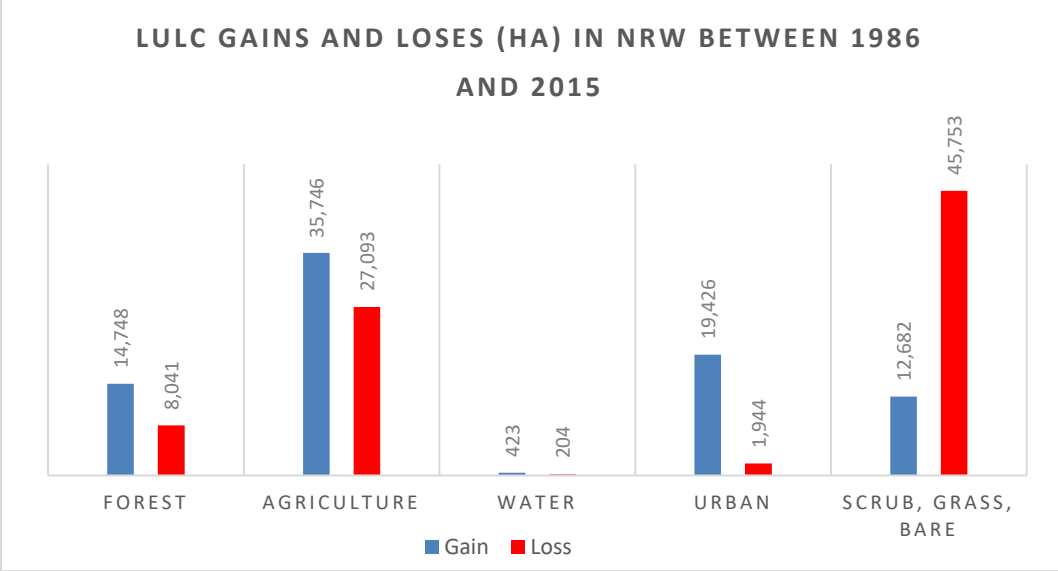

Figure 15 LULC gains and losses between 1986 and 2015

3.3 Geochemistry

3.3.1 Major Elements

The concentration of major oxides, inorganic carbon and sulfur did not change abruptly along Nairobi River gradient. There was no significant pattern to suggest any increase or decrease in the intensity of this group as the river flowed through the different LULC classes. However, there was a weak decreasing trend of Al_2O_3 down the river gradient (Figure 16 and 17). Table 3

below presents the distribution of major oxides, inorganic carbon and sulfur down the gradient of Nairobi River. It is worth noting that the trend of Na_2O and K_2O down the river gradient followed an identical pattern. This is because Na and K are both group one (alkali) metals in the periodic table and therefore they exhibit similar chemical reactions.

Table 3 Distribution of major elements down Nairobi River gradient

Sample	Distance (Km)	SiO_2 %	Al_2O_3 %	Fe_2O_3 %	CaO %	MgO %	Na_2O %	K_2O %	MnO %	P_2O_5 %	C %	S %
NR7	0	55	16.9	9.44	0.49	0.2	2.96	2.82	0.25	0.14	2.29	0.03
NR6	9.14	53.4	16.35	8.64	1.01	0.64	1.41	1.62	0.36	0.11	1.06	0.02
NR5	14.67	42	15.7	9	1.61	0.52	1.43	1.6	0.24	0.77	7.81	0.47
NR4	18.63	45.2	17.3	9.63	1.45	0.51	1.63	1.79	0.29	0.59	5.68	0.28
NR3	31.01	50	15.8	9.88	0.98	0.46	2.11	2.3	0.52	0.52	4.67	0.08
NR2	45.1	58.4	15.55	7.51	1.19	0.44	2.78	2.73	0.26	0.17	1.27	0.13
NR1	47.21	57.8	12.6	9.78	1.61	0.41	2.7	2.75	0.68	0.41	2.42	0.12
MR1	-	39.5	12.15	7.1	2.16	0.54	1.81	2.03	0.24	0.79	13.15	0.43

There was a noticeable difference between the concentration of major elements in samples collected along Nairobi River and the only sample collected in Mathare River (MR). The Mathare River channel's sediment recorded the least concentration of SiO_4 (39.5%), Al_2O_3 (12.15%) and Fe_2O_3 (7.1%). On the other hand, the Mathare sample recorded the highest values for inorganic carbon (13.15%) while the highest concentration of carbon in NR was NR5 (7.81%). This elevated level of inorganic carbon is probably associated with the vegetation characteristics of the catchment and/or the banks of MR in the higher reaches. CaO was also very high in the MR sample than any of NR samples.

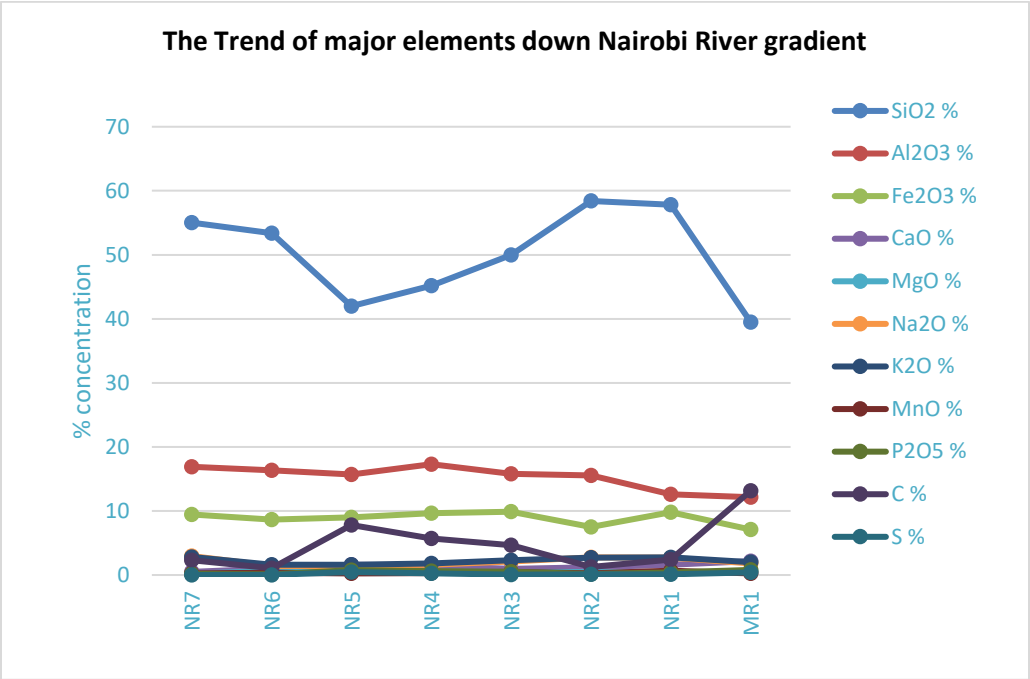

Figure 16 Distribution of major elements down the river gradient

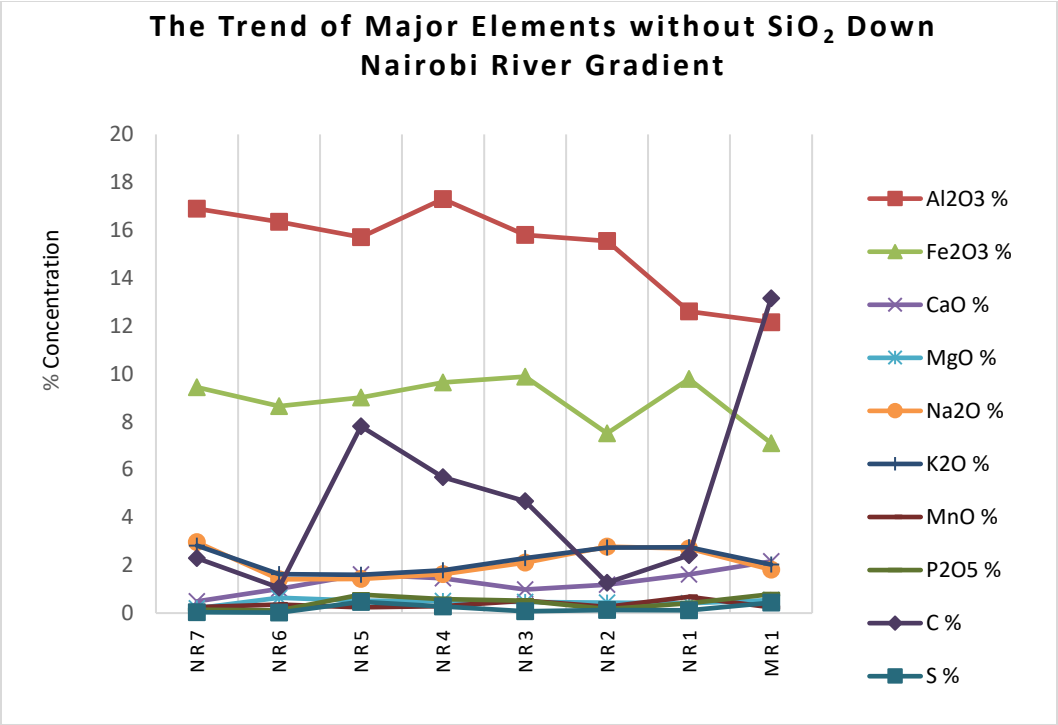

Figure 17 Distribution of major elements without SiO_2

3.3.2 Trace Elements

Trace elements revealed a different pattern, unlike the major elements that had no apparent change down the river. There was a definite increase in the concentration of trace elements down the river gradient. The highest concentrations were recorded in samples collected from the urban class and the concentrations reduced in the samples collected outside the city (see Figure 18 and Table 4 below). There was an increase in the concentration of all heavy metals considered (Sn, As, Hg, Sb, Ag, Cu, Ni, and Pb) in NR3 (urban class). MR1 sample was corrected from within the urban class but from a different river and had the second highest concentration of Cu after NR3. Lead and antimony recorded the highest intensity at 3400 ppm and 187.5 ppm respectively in NR3. Antimony increased by more than 100 times and Pb by about 41 times in NR3 than in the sample with the second highest values.

Table 4 Concentration of heavy metals in ppm

SAMPLE NAME	Distance (Km)	LULC	Sn	As	Hg	Sb	Ag	Cu	Ni	Pb
NR7	0	Agriculture	12	3.3	0.044	0.41	0.25	11	11	44
NR6	9.14	Agriculture	7	2.9	0.03	0.22	0.25	10	20	33
NR5	14.67	Agriculture/Urban	8	3.4	0.082	0.77	0.25	34	19	44
NR4	18.63	Agriculture/Urban	10	3.5	0.107	0.77	0.25	38	21	52
NR3	31.01	Urban	80	22.5	0.564	187.5	3.9	87	30	3400
NR2	45.1	Scrub/grass/bare	9	1.9	0.076	0.65	0.5	26	12	60
NR1	47.21	Scrub/grass/bare	19	4.5	0.219	1.85	0.5	34	17	83
MR1	-	Urban	9	4.5	0.344	1.52	0.8	66	16	65
Correlation coeff' 1			0.25	0.18	0.40	0.18	0.26	0.39	0.07	0.19
Correlation coeffi' 2			0.78	0.80	0.85	0.79	0.79	0.94	0.96	0.79

Table 4 shows the concentrations of some of the trace elements in parts per million (ppm) analyzed from 7 sediment samples collected from five different LULC types in Nairobi River and 1 from Mathare River (MR). Correlation co-efficient 1 compares the concentration of heavy metals to the entire distance sampled along the river while 2 compares the same up to and including the urban class (NR3).

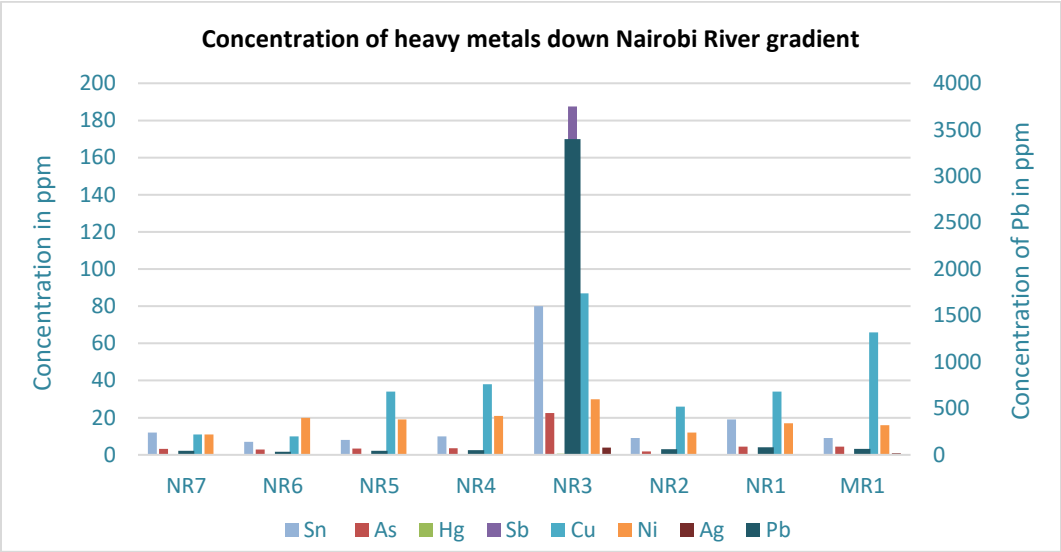

Figure 18 Distribution of heavy metals

This graph presents the distribution of trace elements down Nairobi River gradient, with lead displayed on secondary axis to the right.

To understand these concentrations better, table 5 below compares the highest, lowest and the average concentrations from each sample to the USEPA risk based (RB) soil screening levels (SSL) for the protection of groundwater. Table 5 also shows the detection ratios (DR) of elements which is the ratio of detected concentration divided by the USEPA soil screening levels.

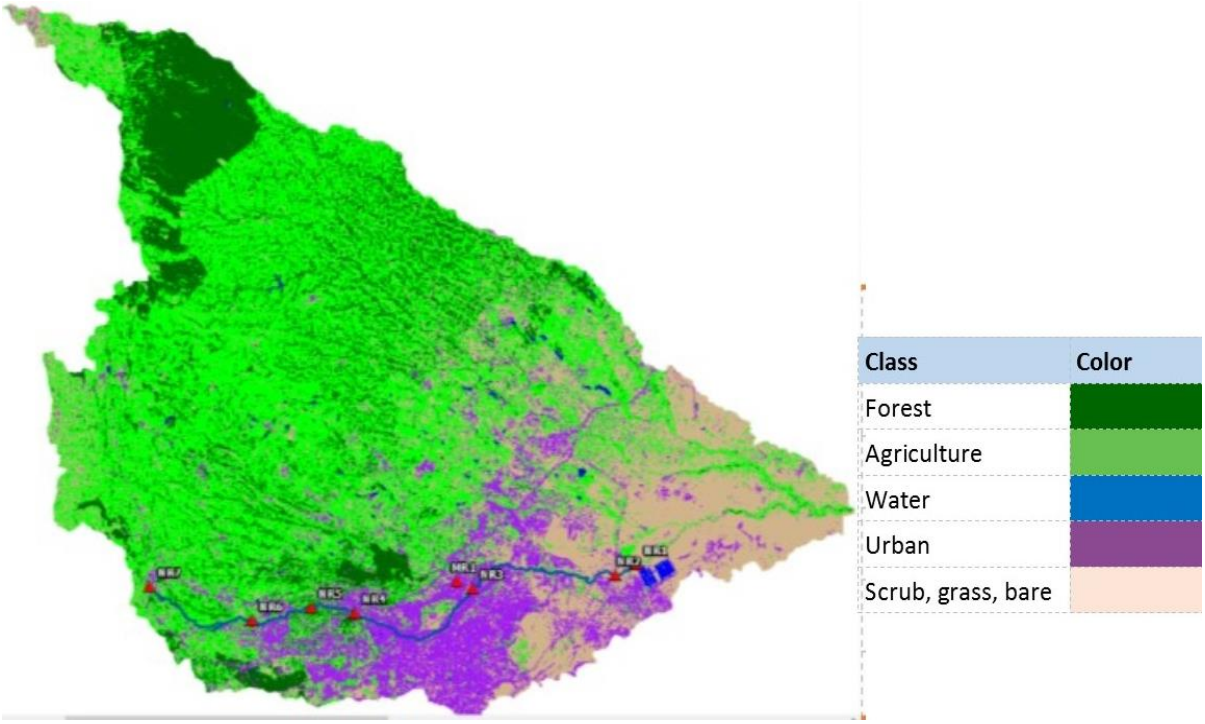

Figure 19 LULC and samples collection points

Figure 19 displays a classified Landsat 8 OLI image of Nairobi River Watershed in May 2015, the length of the River sampled and the samples collection points.

A detection ratio (DR) of 22,700 was recorded for lead in NR3 and 220 in the lowest sample (NR6). As recorded a high DR of 15,000 in NR3 (urban) and a low of 1930 in NR2 (scrub/grass/bare). The highest detection ratio for Sb was 536 from NR3 and the lowest was 0.629 from NR6. Cr recorded a high DR of 9000 and a low of 3000 while Cd had a high DR of 1 and a low of 0.36. Ni and Cu had high DRs of 115 and 3 respectively and low of 4 and 0.3 respectively. Sn had the lowest DR of 0.03 for the sample with the highest concentration and a low of 0.002. The urban class (NR3) recorded all the high DRs while NR6 (agriculture) and NR2 (scrub/grass/bare) recorded the lowest (Table 5).

Table 5 Concentration of primary heavy metals in ppm

Element	Highest	Lowest	Average	EPA RB SSL	Highest DR	Lowest DR
Sn	80	7	19.25	3000	2.67E-02	2.33E-03
As	22.5	2.9	5.81	0.0015	1.50E+04	1.93E+03
Hg	0.564	0.03	0.18	0.018	3.13E+01	1.67E+00
Sb	187.5	0.22	24.21	0.35	5.36E+02	6.29E-01
Ni	30	11	18.25	0.26	1.15E+02	4.23E+01
Pb	3400	33	472.63	0.15	2.27E+04	2.20E+02
Cd	0.75	0.25	0.35	0.69	1.09E+00	3.62E-01
Ce	769	237	444.75	-	-	-
Cr	90	30	50	0.001	9.00E+03	3.00E+03
Cu	87	10	38.25	28	3.11E+00	3.57E-01

Table 5 shows the concentrations of primary heavy metals in ppm, the EPA RB (Risk Based) SSL (Soil Screening Levels) for the protection of groundwater (https://semspub.epa.gov/work/HQ/197025.pdf) and the detection ratios. The EPA values are given in mg/Kg which is equivalent to ppm (1 mg/Kg = 1 part/million). The table presents the highest recorded concentration, the minimum, the average of all records and the USEPA limits. The table also shows the detection ratios (DR) of the samples with the highest and the lowest concentration.

The highest concentration of heavy metals contamination was observed in the samples from the urban classes. For instance, tin concentration increased by eight times from 10 ppm in NR4 to 80ppm in NR3. In this section, Pb increased from 52 ppm to 3400 ppm a two order of magnitude increase or more than 65 times the previous sampled section. The intensity of all the trace elements increased between NR4 and NR3 by about 1.5 times to 65 times. Figure 20 a, and b, shows the concentration of elements down the river gradient. Lead increased the most, and therefore it is plotted separately on a logarithmic scale along the vertical axis in Figure 20b. Similarly, there was a big decrease in heavy metals' concentration between NR3 sample and the next (NR2) down the river gradient.

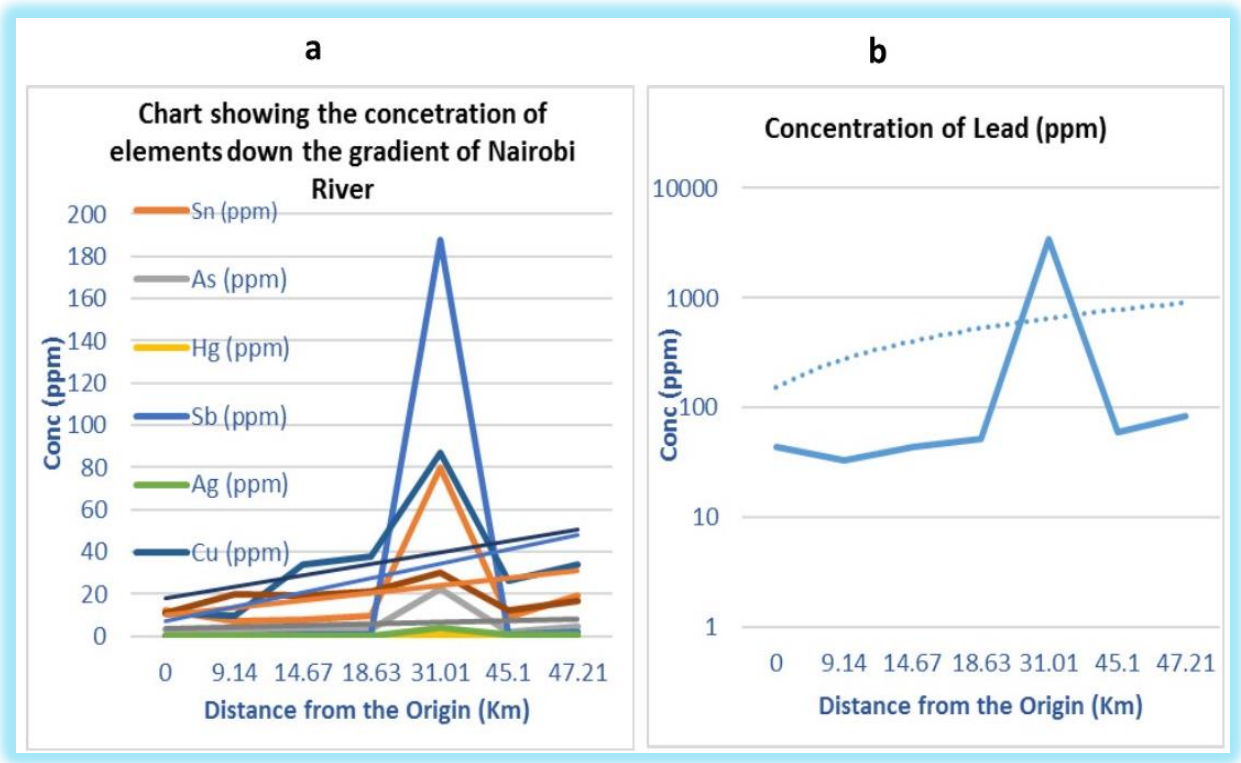

Figure 20 Concentration of trace elements down the river gradient

Figure 20 a, and b, show an increasing concentration of trace elements down the river gradient. Figure 20 b is on logarithmic scale in the vertical axis because of higher differences in concentration of lead.

The trends in figures 20 a, and b, show an increasing concentration of heavy metals down the gradient of Nairobi River for most of the trace elements analyzed. These trends suggest a gradual introduction of heavy metals as the river flow down the gradient. Concentrations of other elements like As, Hg and Ag were relatively constant down the river except at NR3 sample that peaked for all elements. There was a significantly high correlation between the concentration of heavy metals and the distance along the gradient of the river up to and including the urban class. The concentration reduced considerably after the river passed the urban class. The correlation coefficient of the levels of Sn, As, Hg, Sb, Ag, Cu, Ni, and Pb and the distance along the river up to the city ranged between 0.78 and 0.96. However, this correlation coefficient reduced to between 0.07 and 0.4 when the whole section of the river sampled was considered.

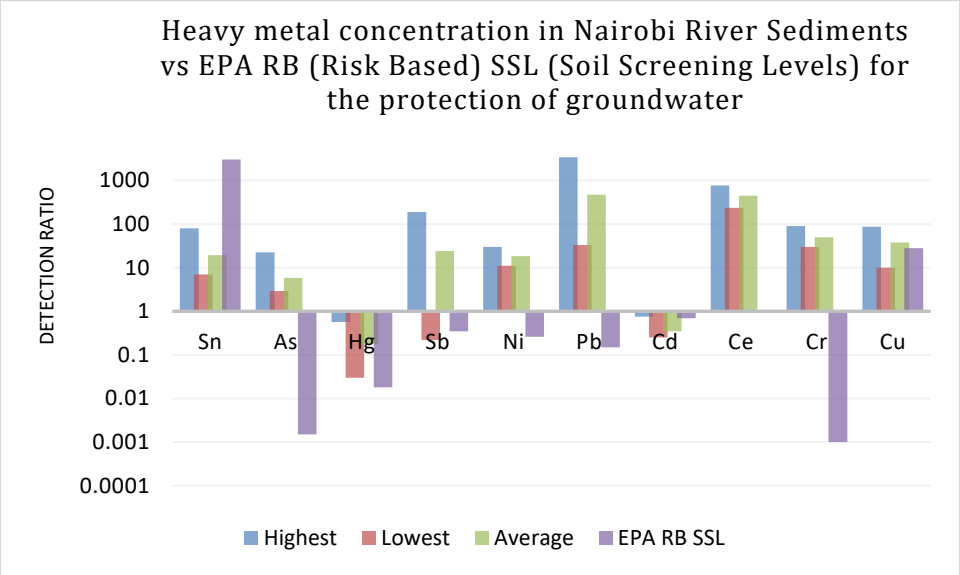

Figure 21 Comparison of concentration of heavy metals to allowable limits

Figure 21 compares the major heavy metals with the EPA RB (Risk Based) SSL (Soil Screening Levels) for the protection of groundwater. It shows the relationship between the highest recorded concentration, the minimum, the average of all records and the EPA limits.

3.3.3 Upper Continental Standardized Spider Diagrams

Spider diagrams were used to compare the geochemistry of NR with the upper continental crust (UCC) for major and rare earth elements (REE). These diagrams are essential for determining enrichment and depletion ratios of elements in comparison to the UCC values. Juvenile UCC ranges were adopted from Condie (1997) because these match well with the geochronology of Nairobi River watershed's igneous material which dates to about 5 million years ago.

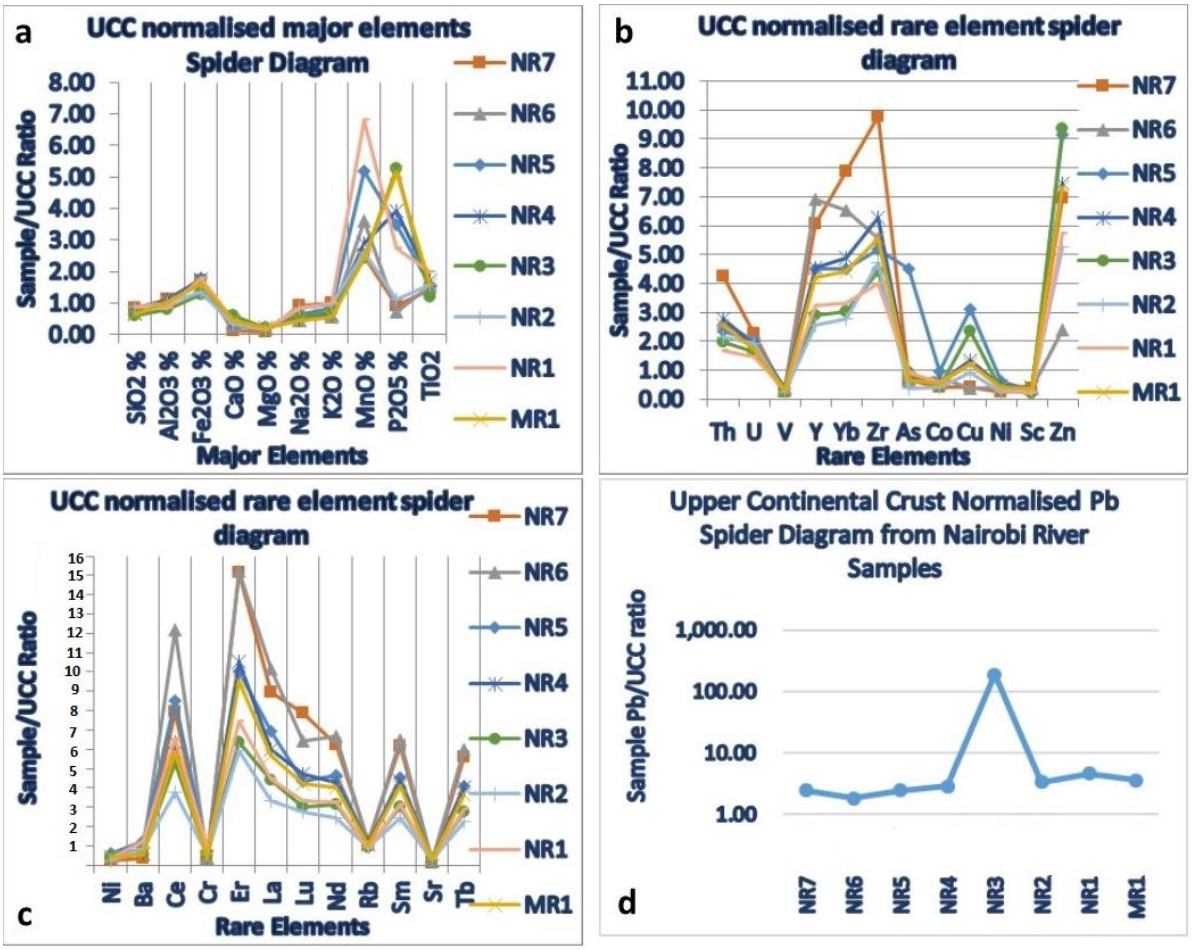

Figure 22 Enrichment/depletion of selected elements against the UCC values

Figure 22 shows Spider diagrams displaying the ratios of enrichment/depletion of selected elements in comparison to the juvenile upper continental crust's values (a) shows the major elements (b) and (c) show rare earth elements and (d) represents Pb distribution.

From Figure 22a above, oxides of Si, Ca and Mg from all the samples exhibited depletion from that of the juvenile UCC values. Oxides of Al, Na, and K, were just about equal values with the UCC values, while those of Fe, Mn and, Ti were conspicuously enriched in all the samples. Phosphate oxides behaved differently whereby in three samples the enrichment factors were about one while in the rest of the samples, concentration rose to a maximum of about five times more than that of the juvenile UCC. The three samples that exhibited equal concentration of P_2O_5 to that of the UCC were picked from near the source of the River, i.e., NR7 and NR6, and the third one

from NR2 (scrub/grass/bare). MnO also behaved like P_2O_5 in that there was a big disparity among samples ranging from an enrichment factor of 2.4 to 6.8. This inconsistency suggests anthropogenic introduction of Mn and P along the river gradient.

Figures 22 b, and c, present a mixture of light rare earth elements (LREE), heavy rare earth elements (HREE) and other trace elements normalized with the juvenile UCC values. Different elements scored differently in which a good number exhibited depletion. Rb remained about the same concentration to the juvenile UCC while several other elements were significantly enriched. Elements that exhibited depletion included Ni, Ba, Co, Sr, V, and Sc. Arsenic had similar characteristics of depletion except for NR5 sample which had an enrichment factor of 4.5. Cu had a similar trend also, in which two samples were significantly depleted, four showed almost similar concentrations with the juvenile UCC values, while two were enriched from the juvenile UCC values. The rest of the elements in figures 22 b and c, showed varying factors of enrichment ranging from about 2 to 15 times. Er recorded the highest enrichment factor of about 15.2 in NR7 and the lowest of about 7.4 in NR2. Cerium had enrichment factors of between 3 at NR 2 and 12 at NR6, while La recorded enrichment factors of between 3 and 10 with the NR6 sample showing the highest enrichment. Lu was highly enriched at NR7 where it recorded an enrichment factor of about eight times and the least enrichment of three times in NR2. Nd was highly enriched in NR 6 with enrichment factors of between 2.5 and 6.7. Sm and Tb were highly enriched in NR7 and NR6 with enrichment factors of 6.5 and 6 respectively, and lowest in NR2 with enrichment factors of 3.2 and 2.9 respectively. Th and Zr were highest enriched in NR7 with enrichment factors of 4.2 and 9.7 respectively and lowest enriched in NR1 with enrichment factors of 1.68 and 3.98 respectively. Yb and Sn exhibited a wide range of enrichment factors down the river gradient with a high of 7.9 for Yb in NR7 and a high of 9.37 for Sn in NR3. Uranium had enrichment factors of

between 1.5 and 2 for all the samples. Figure 22 d, presents Pb concentrations on a logarithmic scale. Lead exhibited the most conspicuous enrichment factor and the biggest disparity of between 2 and 200. NR3 had the highest concentration of Pb by two orders of magnitude in one sample, while the rest of the samples are within the same order of magnitude.

3.3.4 Chemical index of alteration (CIA) and loss on ignition

Table 6 Comparison of percent weight of main elements, CIA, LOI and Rb in ppm

Sample	Distance	Al_2O3%	Na_20%	Ca0%	K_2O%	CIA %	LOI %	Rb (ppm)
NR7	0	16.9	2.96	0.49	2.82	73	11	103.3
NR6	9.14	16.35	1.41	1.01	1.62	80	14.45	91.1
NR5	14.67	15.7	1.43	1.61	1.6	78	24.6	85.5
NR4	18.63	17.3	1.63	1.45	1.79	78	19.95	92.8
NR3	31.01	15.8	2.11	0.98	2.3	75	16.25	86.5
NR2	45.1	15.55	2.78	1.19	2.73	70	9.62	78.1
NR1	47.21	12.6	2.7	1.61	2.75	64	9.24	70.5
MR1	MR1	12.15	1.81	2.16	2.03	67	31.2	77.4

Table 6 shows percentage weight of main oxides used to compute the chemical index of alteration, the CIA, loss on ignition and rubidium values for seven samples collected along Nairobi River and one from Mathare River.

The highest CIA value of 80% was recorded in sample NR6 (Figure 23 and 24), collected about 9 kilometers from Ondiri Swamp, and the lowest CIA was 64% from the last part of the river sampled about 47 kilometers from the origin of the river. The average CIA was 74% which is a little higher than the world's rivers CIA average value of 72% (Li and Yang, 2010). The concentrations of trace elements like niobium and rubidium are also important indicators of alteration (Price and Velbel, 2003; Krissek and Kyle, 2001).

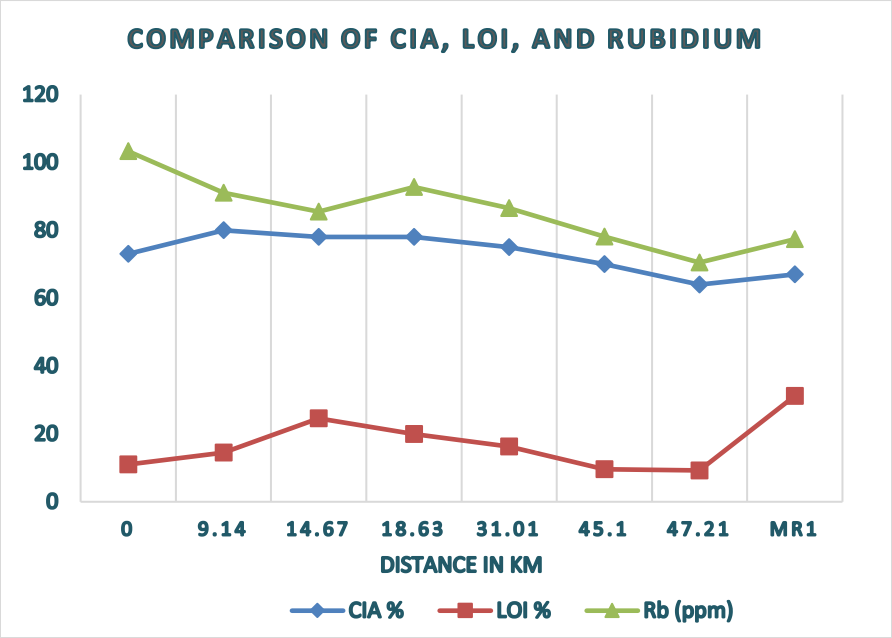

Figure 23 Relationship between CIA, LOI and Rubidium

The trend of Rb concentration along Nairobi river matched that of CIA in all samples except one (Figure 23). Higher concentration of rubidium and niobium indicate greater alteration of the soil from the parent material while low levels of these trace elements indicate less alteration from the parent material. Similarly, CIA values are an indication of soil alteration from the parent material in which high values of CIA suggest a greater level of weathering. The trend of Loss on ignition also appeared to correspond very well with both the CIA and Rb concentration. Out of the eight samples analyzed, seven samples correlated very well with LOI and CIA and only NR5 (14.67 Km from the origin) increased while CIA was decreasing.

In Figure 24, rare earth elements were plotted together with the CIA values to determine the relationship in their trends along the river. This figure shows the comparison of the ratios of the summation of light rare earth elements to the heavy rare earth elements (LREE/HREE), lanthanum to ytterbium (La/Yb) and CIA. Lanthanum is a light rare earth element while ytterbium

is a heavy rare earth element. This ratio is also a tool used to indicate weathering in soils. The lower mobility of LREE (light rare earth elements) relative to HREE (heavy rare earth elements) results in the enrichment of LREE and depletion of HREE (Cao et al. 2016). In highly weathered soils, the ratio of LREE to HREE is expected to be higher than in less weathered soils. This ratio would be expected to be similar to that of the ratio of lanthanum a LREE to ytterbium a HREE. For highly weathered soils, La/Yb ratio would be greater than in the less weathered soils.

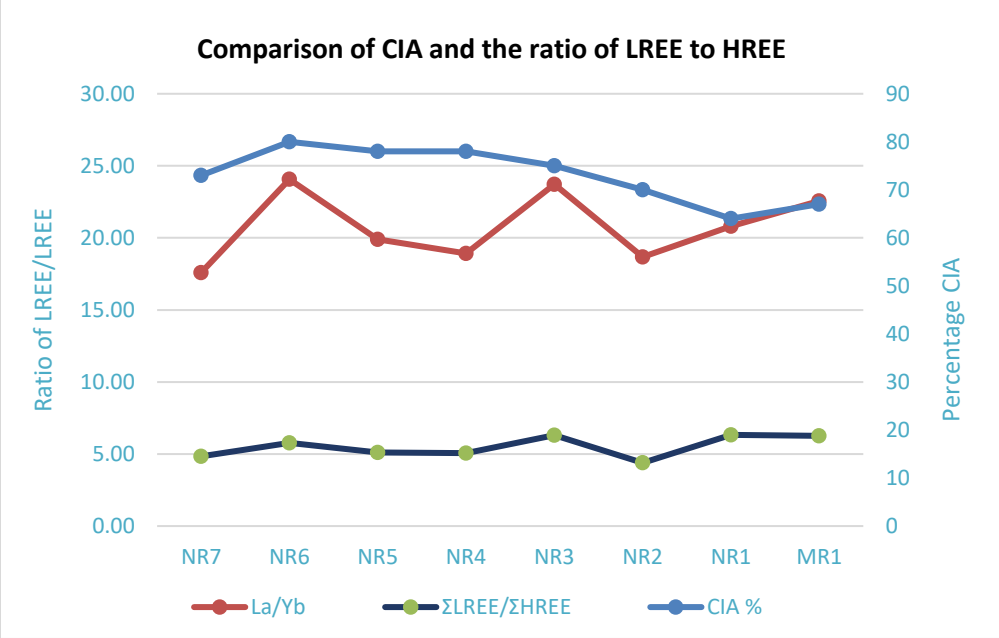

Figure 24 Comparison of CIA, LREE/HREE and La/Yb ratios

NR6 had the highest CIA (80%), and therefore it is assumed to be highly weathered than the rest of the samples (Figure 23 and 24). This CIA coincided well with both the ratios of LREE/HREE and La/Yb which also showed high values in this sample. The trend of the ratios of light to heavy rare earth elements was very similar to that of CIA except in two cases. NR3 showed decreasing weathering in comparison to the previous sample (NR4) according to CIA, but the ratios of LREE/HREE and La/Yb showed an increased weathering activity in NR3 than NR4. NR1

also depicted a decreased weathering rate than NR2 according to CIA while LREE/HREE and La/Yb indicated an increased rate of weathering. Other samples, i.e., NR7, NR6, NR5, NR4, NR2, and MR1 agrees well with Cao et al. (2016).

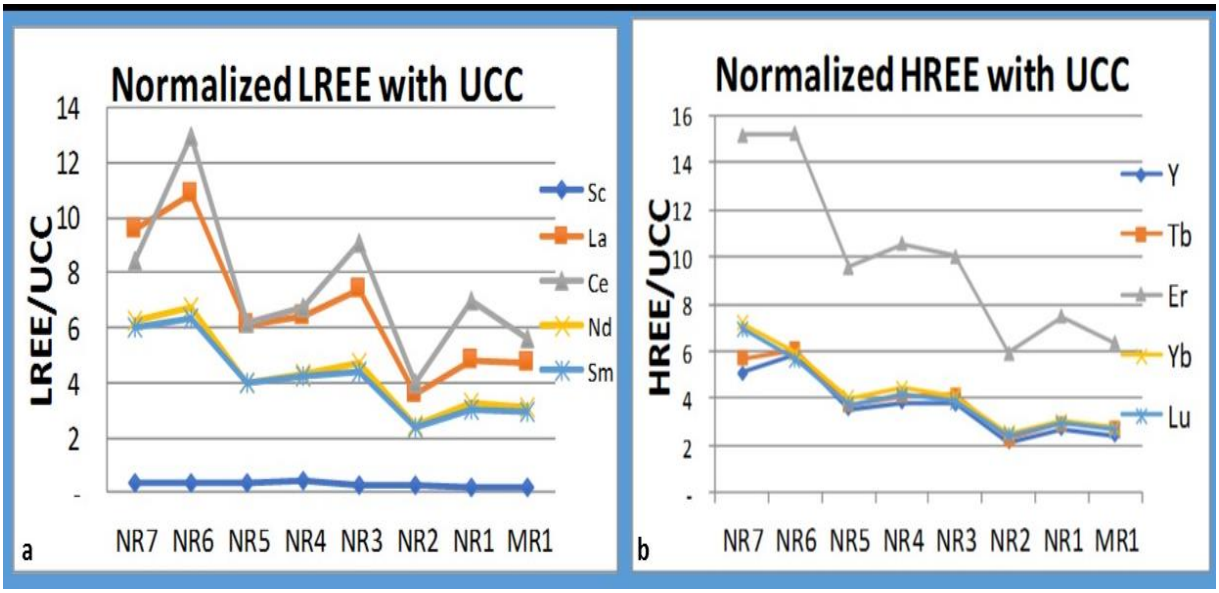

Figure 25 The general trend of REE along the river gradient

These graphs present the general trend of a, LREE (light rare earth elements) and b, HREE (heavy rare earth elements) along the river gradient

Figure 25 shows a decreasing trend for the normalized LREE and HREE to that of the juvenile UCC values down the river gradient. All the REE elements analyzed revealed a decreasing trend of the normalized index with the juvenile UCC as the river flowed down the gradient.

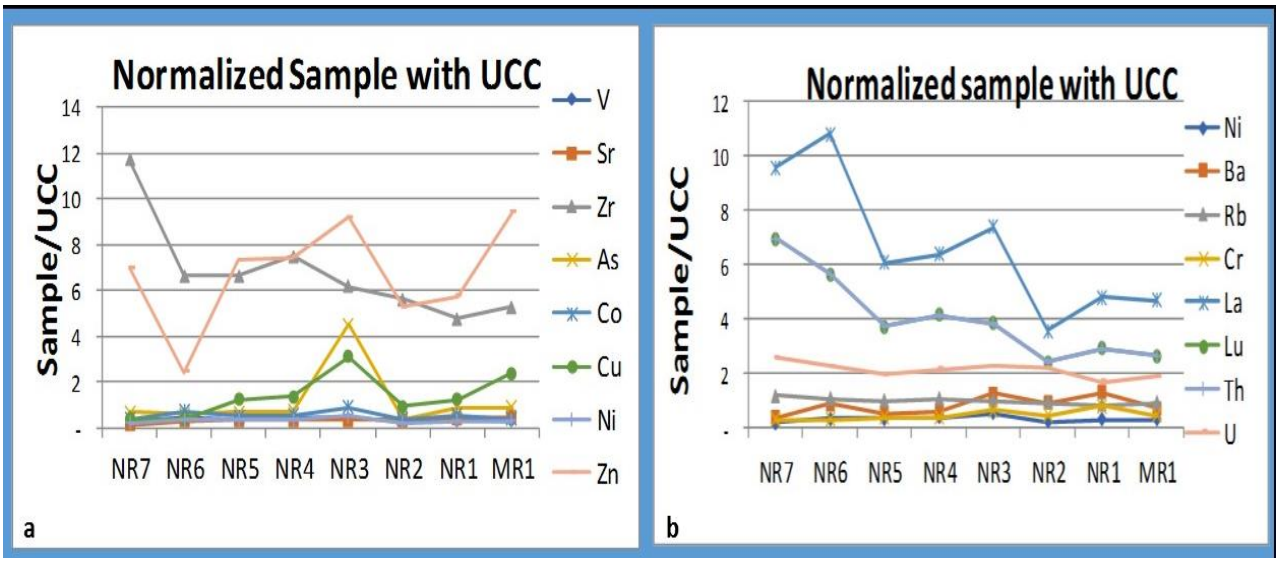

Figure 26 General trend of Sample elements/UCC down river gradient

Most of the elements had a remarkable decrease of the normalized index to the juvenile UCC values down the river gradient. Some elements that exhibited this decrease were zirconium, lanthanum, lutetium, thallium, uranium, and rubidium. Zinc and copper increased convincingly down the river gradient while barium increased marginally (figure 26 a and b). Elements that were always below the UCC level, i.e., having a ratio of less than one, exhibited little change down the river gradient. It is also worthy to note from figure 25 and 26 the relationship of some trace elements depending on the trend exhibited by their curves. LREE elements, i.e., La, Ce, Nd and Sm; and HREE, i.e., Y, Tb, Yr, Er, and Lu exhibited almost an identical trend of enrichment down the river, but with varying enrichment factors.

3.4 Mineralogy

3.4.1 Bulk Minerals

Table 7 Bulk mineral composition

Sample	001 peak (Å)	002peak (Å)	003peak (Å)	004peak (Å)	ID	Semiquant %
MR1	4.24 - 4.25	3.33-3.35	2.45-2.46	2.27-2.28	Quartz low	19
	6.5	5.8	4.5	4.1	Anorthoclase	81
NR1	4.24-4.26	3.34	2.45-2.46	2.28	Quartz low	22
	6.45-6.48	5.78-5.83	4.46-4.5	4.09-4.1	Anorthoclase	78
NR2	4.24-4.25	3.34	2.46	2.28	Quartz Low	13
	6.45-6.48	5.8-5.82	4.45-4.47	4.1	Anorthoclase	87
NR3	4.24-4.25	3.34	2.45-2.46	2.28	Quartz Low	20
	6.44-6.48	5.8-5.81	4.45-4.46	4.09-4.1	Anorthoclase	80
NR4	4.23-4.25	3.33-3.34	2.45-2.46	2.28	Quartz Low	21
	6.43-6.48	4.45-5.84	4.1-4.45	4.04-4.1	Anorthoclase	79
NR5	4.23-4.27	3.33-3.35	2.44-2.46	2.26-2.29	Quartz Low	24
	6.44-6.52	5.78-5.79	4.45-4.48	4.1-4.11	Anorthoclase	74
	4.12	2.52	2.15	2.01	Cristobalite?	2
NR6	4.25-4.26	3.33-3.36	2.44-2.45	2.28	Quartz Low	20
	6.49-6.5	3.33-3.36	4.55-4.56	2.28	Anorthoclase	80
NR7	4.24-4.26	3.33-3.35	2.45	2.28	Quartz Low	18
	6.44-6.45	5.77-5.8	4.55-4.57	4.1	Anorthoclase	78
	4.03	2.84	2.33-2.48	2.21-2.46	Cristobalite?	4

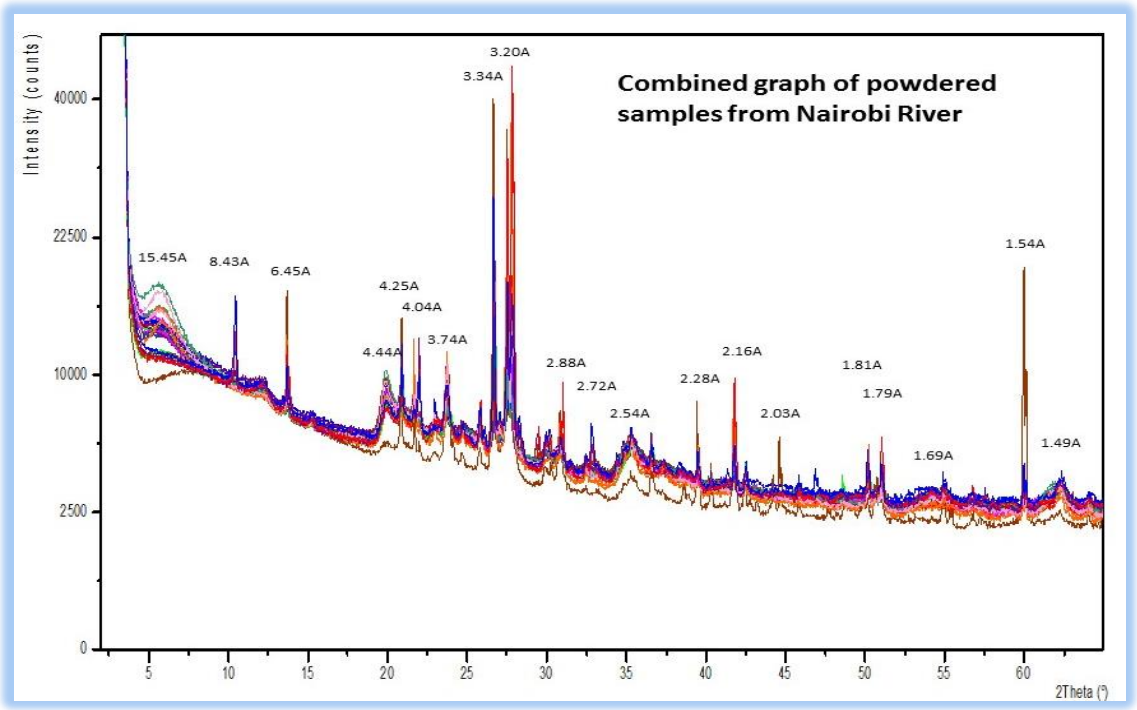

Figure 27 XRD peaks for combined bulk mineralogy

The bulk mineral analysis was carried out on fine powder from different sediment fractions where theta was set to run from 0.5º to 60º, and the XRD generator set at 45kV tension and 40kA current.

The mineral composition of the samples was very similar in all bulk fractions with a little exception in a couple of samples. Quartz and anorthoclase were the dominant minerals in all the samples and cristobalite probably appearing in only a couple of samples at very low quantity (Table 7 and Figure 26). Quartz mineral is second after feldspar in abundance on the Earth's Crust. It is a continuous mineral composed of silicon and oxygen (SiO_4) atoms forming a silicon-oxygen tetrahedral structure. Anorthoclase ((Na, K)Al Si_3O_8) is a crystalline mineral of feldspar series in which sodium-aluminum silicate member is abundant than the potassium-aluminum silicate member, i.e., $NaAlSi_3O_8$ occupies 64-90% while $KAlSi_3O_8$ occupies 10-36% of the structure. Cristobalite mineral was detected in two samples, i.e., NR5 and NR7. Cristobalite is a high-

temperature polymorph of silica and has the same chemical formula as quartz but with a different crystal structure. Quartz and cristobalite are both members of the quartz group.

3.4.2 Clay Minerals

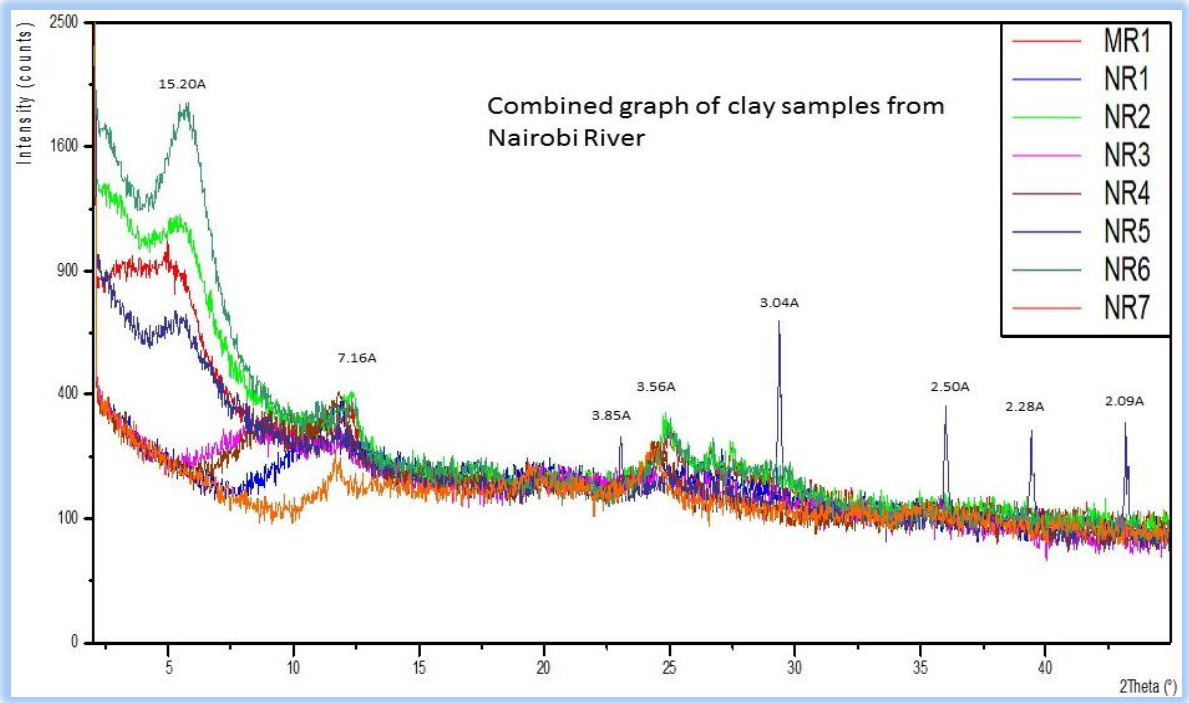

Figure 28 XRD peaks for combined clay mineralogy

Clay minerals' analysis was done from air dried samples on petrographic microscope slides and theta running from 0.5° to 45° and the generator set at 45kV tension and 40kA current

Like in the bulk minerals, clay minerals had very similar composition along the river. All the samples except NR1 had a presence of a more >14 Å and a 7 Å clay minerals. These peaks corresponded well with smectite and kaolinite peaks. After application of glycol, the 001 peak for smectite increased in magnitude suggesting an increase in the d-spacing as result of the expansion of the interlayer due to intercalation with glycol. The 001 peak for kaolinite did not change significantly. Upon heating at 550°C for about 1 hour, the magnitude of the 001 peak of smectite reduced significantly while the 001 peak for kaolinite reduced or collapsed (Figure 29). The clay

minerals in Nairobi River sediments were largely composed of smectite and kaolinite minerals (Table 8).

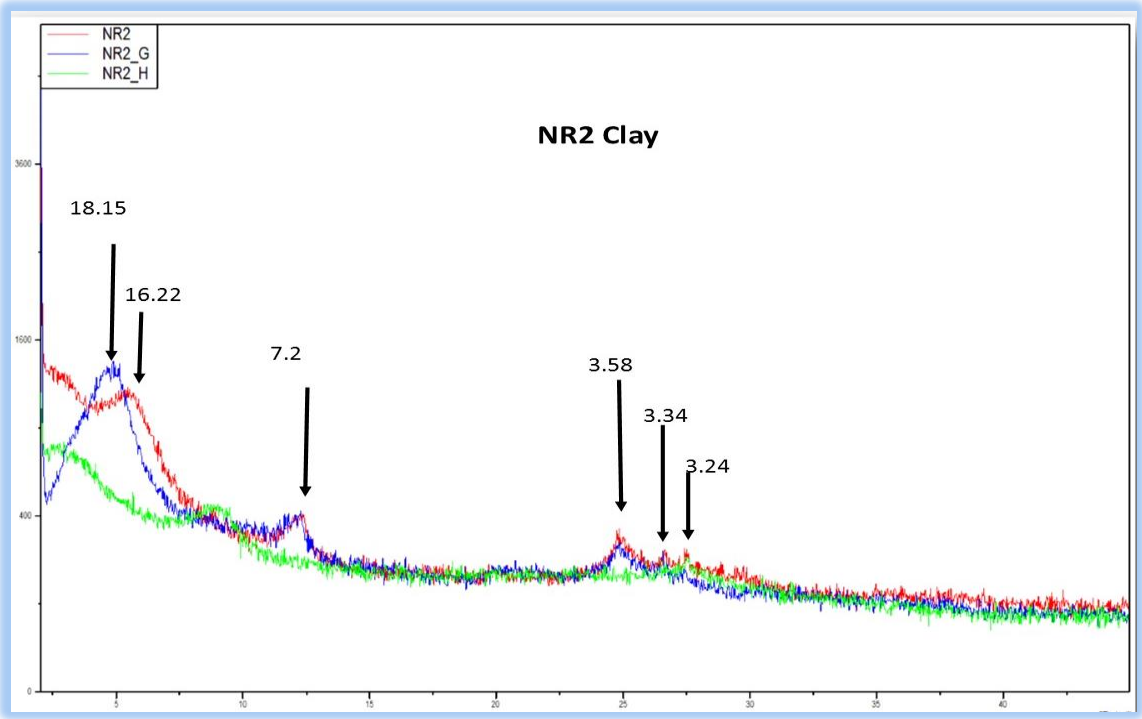

Figure 29 A graph showing air dried, glycolated and heated clay peaks

The red series represents air dried sample, G represents the glycolated one for 24 hrs in glycol vapor, and H the heated sample at 550ºC for about one hour.

Table 8 Clay mineral composition

Sample	Treatment	1st peak	2 nd peak	ID
MR1	Air Dry	17.63	7.2	Smectite, Kaolinite
	Glycol	18.34	7.2	Smectite, Kaolinite
	Heated	10.02		Smectite
NR1	Air Dry	7.6	3.63	Kaolinite
	Glycol	9.31	about 5	
	Heated	13.27		
NR2	Air Dry	16.22	7.2	Smectite, Kaolinite
	Glycol	18.15	>7.2	Smectite, Kaolinite
	Heated	Mid A &G		
NR3	Air Dry			
	Glycol	19.9	7.45	Smectite, Kaolinite
	Heated	13.86		Smectite
NR4	Air Dry	9.75	>7.24	Smectite, Kaolinite
	Glycol	17.39	7.24	Smectite, Kaolinite
	Heated	18.42		Smectite?
NR5	Air Dry	16.6	7.47	Smectite, Kaolinite
	Glycol	18.06	about 7.47	Smectite, Kaolinite
	Heated	<16.6		Smectite
NR6	Air Dry	15.45	7.16	Smectite, Kaolinite
	Glycol	16.76	8.71	Smectite, Kaolinite
	Heated			
NR7	Air Dry	about 7.25		Kaolinite
	Glycol	17.03	7.25	Smectite, Kaolinite
	Heated	10.77		Smectite

Further treatment of air-dried samples to distinguish between the kaolin group revealed that there was no significant amount of halloysite mineral in the clay fractions. The air-dried samples were sprayed with formamide liquid and analyzed within 20 to 30 seconds after the treatment. Upon treatment of the samples with Formamide the 7 Å clay (the kaolin group) was supposed to have a distinct first peak for halloysite if present at around 10 Å region and kaolinite first peak to remain at 7 Å region. There was no significant change between the peaks of the two

treatments, and therefore the main kaolin group present in Nairobi River clay sediments for the sampled locations was kaolinite (see Figure 30).

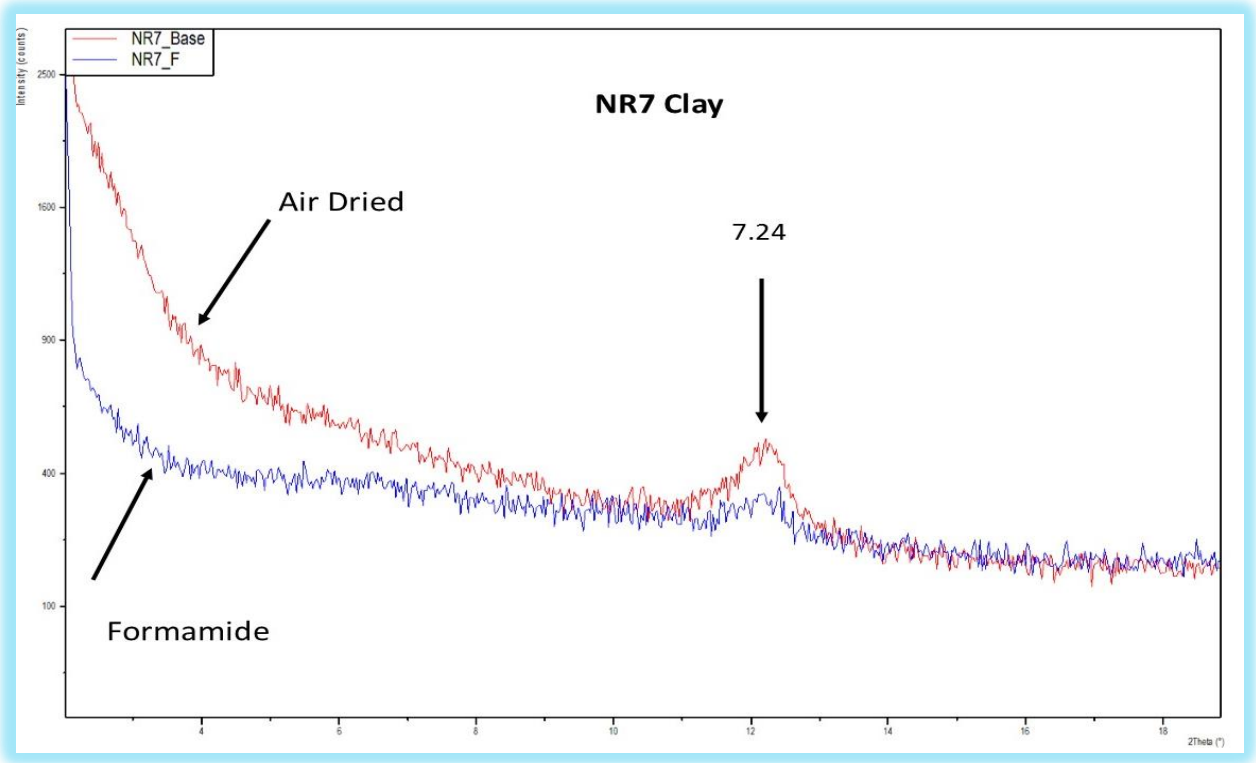

Figure 30 Air dried and formamide treated clay peaks

3.5 Loss-on-Ignition

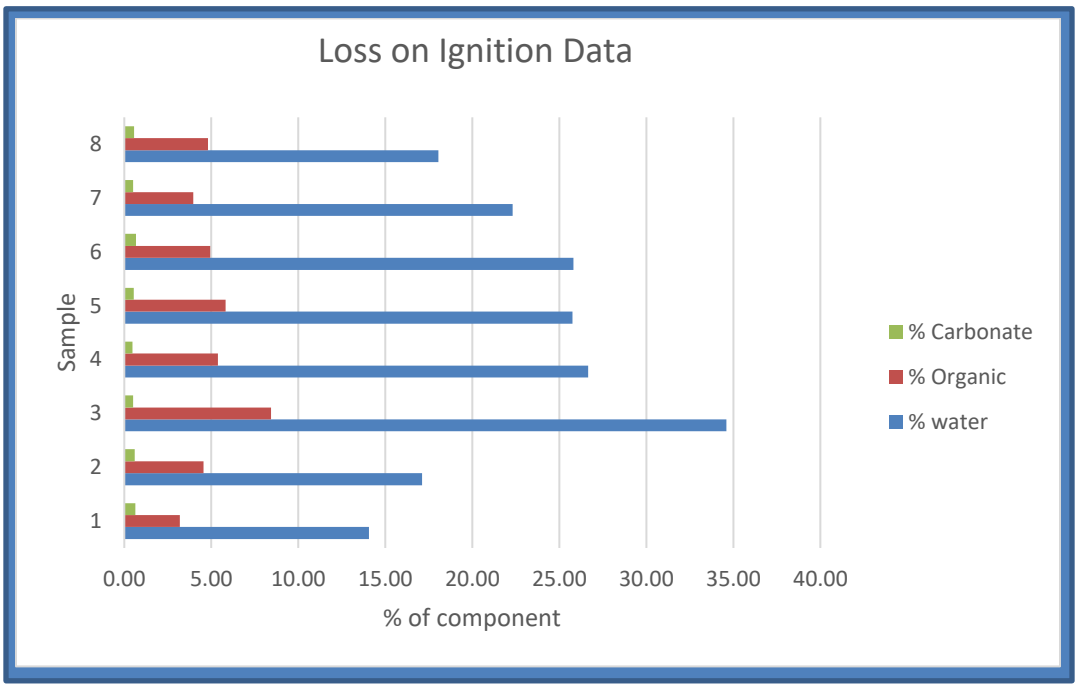

Figure 31 Loss-on-ignition

In Figure 31, sample 1=NR1, 2=NR2, 3=MR1, 4=NR3, 5=NR4, 6=NR5, 7-NR6 and 8=NR7. This is the order in which the samples were collected.

Figure 31 shows the loss on ignition (LOI) graph. There was a constant amount of carbonates in all samples which ranged from 0.47% to 0.63%. The organic matter, however, showed different proportions for all the samples and ranged from slightly above 3% to approximately 8.5% of the total sample. The highest organic matter content was recorded in the only sample collected from Mathare River one of the tributaries of Nairobi River.

4 DISCUSSION

In this study, urban class constituted all man made infrastructure of build land surfaces including roads, buildings, parking areas, pavements etc. Urbanization has been increasing at a relatively high rate in Nairobi River Watershed (NRW) since 1986. It rose from 4,746 ha in 1986 to 22,243 ha in 2015, approximately 17,497 ha increase in 3 decades, about 600 ha increase of

impervious surface every year. Urbanization was the solitary class that had a relatively very low loss compared to the gain throughout the three decades. In projection, by the year 2050, about 41,000 ha of NRW will be an impervious surface which will account for about 22% of the total watershed area, compared to May 2015, which was about 12% impervious surface. Most of the urban expansion happened in the scrub, grass and bare areas and seldom affected the forest class. It is surprising that this study found out that forest cover increased by about 6000Ha over that time period. This increase may be attributed to policy frameworks and agencies like the Kenya Forests Service (KFS) and the Greenbelt Movement, that were formed to conserve and increase land under forest cover in Kenya. The Greenbelt and other non-governmental activists advocated for Karura Forest for decades which was earmarked for deforestation in the 1980s and 1990's to create space for urbanization. In the last 15 to 20 years, farmers in Kenya including in NRW have planted trees plantations especially the fast growing blue gum for business. In this classification this was treated as agriculture but it is also possible that there were pixels that were misclassified as forest instead of agricultural. Change detection image recorded some pixels that were converted from urban to forest and this is could also be a case of pixel misclassification too.

The LULC analysis is critical because there is a good relationship between LULC and the concentration of inorganic pollutants along Nairobi River channel. Urban environment was the most significant contributor of inorganic contaminants than other classes of LULC. A consistent increase of heavy metals down the river gradient occurred from the largely agricultural section of the river, i.e., samples NR7 and NR6 to the urbanized section. These metals had a gradual increase between samples NR5 and NR4 and a sudden rise in sample NR3 which was collected at the center of the city. Sample MR1 was not collected from NR but from Mathare River which is at proximity to sample NR3. The Mathare River sample had a mild concentration of heavy metals, unlike the

NR3, even though they were next to each other. However, the levels of heavy metal pollutants in MR1 sample were significantly above other samples collected outside the more urbanized sections of NR. Sample NR2 was collected from a less build, and more open and bare-ground area and the effects can be seen from the lower concentrations of heavy metals in this sample. There was sudden fall of concentrations between NR3 and NR2, although a considerably long segment of about 14 Km separated the locations of the two samples. Sample NR2 shows that urbanization had the highest contribution to river pollutants, which were adsorbed significantly by soils and clays along the river channel, between samples NR3 and NR2 (Figure 18). There was a very small rise in concentrations of heavy metals in NR1 which was collected at about a couple of kilometers from NR2. This rise is not very large; it may be due to through-flow through the water treatment system, or some other local input. No elevated heavy metals are found downstream, suggesting the system may be performing it's purpose with respect to those contaminants. McCarthy et al. (2017) established a significant statistical relationship between the LULC fractions in Tampa Bay Watershed (Florida) and the water quality. In this study, various segments of the estuaries responded differently to developed land, agricultural land, and bare-land. Urban land-use was the main cause of nutrients concentration increase in the riparian zones of Tropical Region of Brazil (Tromboni and Dodds, 2017). Urban and agricultural lands produced much higher inorganic pollution to surface water in Ohio watersheds than other land surfaces (Tong and Chem, 2002). These observations correspond well with this study, where urbanization was found to contribute more inorganic pollution to NR than other LULC.

The watershed was largely agricultural in both 1986 and 2015 with approximately 86,363 ha, about 46% of total land cover in 2015. There was no proper data to determine the effects of agriculture on the quality of water in the river because the section sampled was either under

farming or urban influence. There was not a good portion of the watershed right from the origin of the river, that was undisturbed by humans, to act as a control sample in determining the anthropogenic impacts on the other sections. The effects of urbanization were solely based on samples from the agricultural sections of the watershed and the bare-ground which probably had the intrusion from urban class by the flowing water. However, it is evident that urbanization in Nairobi River Watershed has adverse effects on water quality than both agricultural and scrub/grass/bare.

Inorganic elements recorded different enrichment factors to that of the juvenile UCC. Some were very uniform down the river gradient while others were very erratic. Inorganic elements that had little to no change down the river gradient were as a result of natural causes rather than anthropogenic sources as observed by Saha et al. (2016). In this study, V, As, Co, Sc, Ni, Ba, Cr, and Sr had an enrichment factor of about one or less and had a very uniform distribution down the river (Figure 22). Elements that exhibited low and homogeneous levels of concentrations and therefore had less standard deviation were likely due to natural sources (Manta et al., 2002). Uranium had a relatively uniform concentration but had an enrichment factor of about 2. On the other hand, Th, Y, Yb, Zr, Cu, Zn, Ce, Er, La, Lu, Nd, Sm, and Tb had very disproportional enrichment factors and were all above one to about fifteen times. These high concentrations coupled with large standard deviations were probably due to anthropogenic introduction (Manta et al., 2002). Major elements were relatively uniformly distributed along the river gradient except magnesium and phosphorous. Elements that exhibited less or no change in concentration down the river gradient like V, As, Co, Ni, Sc, Ni, Ba, Cr, and Sr were probably contributed by natural sources rather than anthropogenic sources (Saha et al., 2016). Other elements that showed great variation in concentration down the river gradient were largely due to anthropogenic sources than

natural causes. The concentration of phosphorous especially PO_4 among other compounds like ammonia and elements like K have been used as indicators of gray water in surface water bodies (Panasiuk et al., 2015). In this study, samples collected within the urban classes had relatively high enrichment factors of the oxides of phosphorous ranging from 1.5 to 5 times. The natural sources of manganese include manganese-bearing minerals like pyrolusite, rhodocrosite, rhodonite, hausmannite, etc. The anthropogenic sources of environmental manganese are wastewater discharge, sewage sludge, mining, mineral processing, fossil fuel combustion, and emission, etc. The mineralogy analysis did not record manganese bearing minerals, and therefore it is probable that Mn was being introduced into the river channel through anthropogenic avenues.

The geochemistry of the river sediments down the gradient suggested that sediments were more altered up the river than at low altitudes. The CIA and the concentration of Rb depicted a decreasing trend of soil alteration, but the ratio between the LREE to HREE did not show any significant trend. The sediments recorded an average CIA value of 74% which is slightly higher than the world river CIA average value of 72% (Li and young, 2010). These CIA values ranged from 67% to 80% and this corresponded well with the clay minerals that recorded high amounts of smectite and kaolinite. These minerals are the end products of clay weathering, and they represent clay particles that are highly altered. The halloysite mineral in kaolin group suggests less weathering and a test for halloysite mineral in the clay fraction returned no significant halloysite minerals present. The weathering indices used suggested that the higher altitude reaches of Nairobi River had more altered soils from the parent materials than the lower altitude segments.

5 RECOMMENDATIONS AND CONCLUSION

This study revealed a dynamic watershed whereby urbanization increased by about 17,497 Ha (369%); agriculture increased by about 8,618 Ha (11%) while forest cover rose by about 6,679 Ha (26%). Most of the area under scrub/grass/bare was converted into agriculture and urban classes whereby the scrub/grass/bare class decreased coverage by 33,071Ha (42%). There was a positive correlation between the type of LULC and the quality of water in Nairobi River. The geochemistry of the channel sediments changed considerably as the river flowed from the less urbanized and more agricultural landscape to a more urbanized landscape and out into a sparsely developed area. The concentration of heavy metals in the urban class was way above that of other classs. Heavy metals of concern, e.g., As, Hg, Sb, Pb, etc., recorded high values in NR3 sample which is an indication that anthropogenic activities along the river in the city were affecting the geochemistry of Nairobi River (Figure 20 a, and b,). The MR1 sample was equally elevated compared to other samples collected from lesser developed locations. This sample was also obtained from an urban class but from a different river, i.e., Mathare River (Figure 18). There was a good correlation between the intensity of contaminants (heavy metals) and the distance of the river from the origin up to and including the highly urbanized section (Table 4 and Figure 18). Analysis of the CIA and the rare earth elements revealed dynamic soil alteration levels but mainly decreasing down the gradient (Figure 23 and 24). Lastly, this study demonstrates that the concentration of inorganic contaminants along a river channel can be a useful geochemical tracer to monitor anthropogenic activities in a watershed.

There is a need to consider proper urban planning in future because of the rate of urbanization observed for the past three decades and the predictions to the future. Environmentally friendly constructions like green-roofs, floodwater seepage zones, protection of groundwater recharge zones and river buffers are therefore highly recommended. This study suggests that

policies promoting forests' protection have been successful in NRW and these should continue into the future. Moreover, future urban planning should work on minimizing impervious surfaces as much as possible, protect forests coverage and increase the area under the tree canopy. The urban class was the highest contributor of inorganic contaminants in the river channel, and therefore proper waste disposal channels should be encouraged. There should be amicable steps to reduce and eradicate point source pollution getting into the river system. Adequate measures should be put in place to address the effects of diffused pollutants into the river by stormwater.

REFERENCES

African Development Bank, 2010. Nairobi rivers rehabilitation and restoration program: sewerage improvement project. Project appraisal report. Nairobi: African Development Bank Group.

Alphan, H., 2003. Land-use Change and Urbanization of Adana, Turkey. Land Degrad. Dev.14:575–586

Alvarez-Cobelas, M., Angeler, D.G., Sánchez-Carrillo, S., 2008. Export of Nitrogen from Catchments: A World-Wide Analysis. Environ Pollut. 156:161–169

ANZECC, 2000. Australian Water Quality Guidelines for Fresh and Marine Waters, Australian and New Zealand Environment and Conservation Council, Kingston.

Arnold, C.L., and Gibbons, J.C., 1996. Impervious Surface Coverage: The Emergence of a Key Environmental Indicator. The American Planning Association. 62:243-258.

Athi Water Services Board: Projects, 6 November 2011

ATSDR, 1999. Toxicological Profile for Cadmium. Atlanta, GA: Agency for Toxic Substances and Disease Registry.

Baker, B.H., Mitchell, J.G., and Williams, L.A.J., 1988. Stratigraphy, Geochronology and Volcano-Tectonic Evolution of the Kedong-Naivasha-Kinangop Region, Gregory Rift Valley, Kenya. Geological Society [London].145:107-116

Barkhordari, J., Vardanian, T., 2012. Using Post-Classification Enhancement in Improving the Classification of Land Use/Land Cover of Arid Region (A Case Study in Pishkoush Watershed, Center of Iran). Range Sci. 2 (2):459-463

Cao, L., Zheng, M., and Caldeira, K., 2016. Simulated Effect of Deep-Sea Sedimentation and Terrestrial Weathering on Projections of Ocean Acidification. Geophysical Research. 121:2641-2658

Chithra, S.V., Harindranathan, M.V., Amarnath, A., Anjana, N.S., 2015. Impacts of Impervious Surfaces on the Environment. International Journal of Engineering Science Invention. 4 (5):27-31

Cihlar, J., and Jansen, L.J.M., 2001. From Land Cover to Land Use: A Methodology for Efficient Land Use Mapping Over Large Areas. Association of American Geographers. 53 (2): 275-289

Condie, K.C., 1997. Plate Tectonics & Crustal Evolution. 4th Ed. New Mexico Institute of Mining and Technology Socorro, New Mexico

Coskun, H.G., Tanik, A., Alganci, U., Cigizoglu, H., 2008. Determination of Environmental Quality of a Drinking Water Reservoir by Remote Sensing, GIS and Regression Analysis. Water, Air, and Soil Pollution. 194:275-285.

Cullen, W.R., and Reimer, K.J., 1989. Arsenic Speciation in The Environment. Chem. Rev. 89:713-769

Daily Nation, Kenya, Tuesday September 27, 2016. http://www.nation.co.ke/counties/nairobi/polluted-Nairobi-rivers-clean-up/1954174-3396194-su6tug/

Defra, 2012. Tackling Water Pollution from the Urban Environment. Consultation Report. Dept. of Environment & Food & Rural Affairs (Defra), London, UK (November 2012).

DeMer, M.N., 2005. Fundamentals of Geographic Information Systems. 3rd ed. NY

Dwivedi, R. S., Sreenivas, K., & Ramana, K.V., 2005. Land-Use/Land-Cover Change Analysis in Part of Ethiopia Using Landsat Thematic Mapper Data. International Journal of Remote Sensing. 26(7)

El-Bouraie, M.M., El Barbary, A.A., Yehia, M.M., Motawea, E.A., 2010. Heavy Metal Concentrations in Surface River Water and Bed Sediments at Nile Delta in Egypt. Suo 61 (1):1–12.

El-Kowrany, SI., El-Zamarany, E.A., EL-Nouby, K.A., El-Mehy, D.A., Ali, E.A.A., Othman, A.A., Salah, W., and EL-Ebiary, A.A., 2016. Water Pollution in The Middle Nile Delta, Egypt: An Environmental Study. Advanced Research 7:781-794

Engineering and Consulting Firms Association, Japan Nippon Koei Co., Ltd. (March 2008). "Project Formulation Study on Nairobi Metropolitan Development Planning Project" . p. 11. Retrieved 7 November 2011.

Fedo, C.M., Nesbitt, H.W., Young, G.M., 1995. Unraveling the Effects of Potassium Metasomatism in Sedimentary Rocks and Paleosols, With Implications for Paleo-Weathering Conditions and Provenance. Geology. 23: 921–924

Foody, M.G., 2002. Status of Land Cover Classification Accuracy Assessment. Remote Sensing of Environment. 80:185-201

Foster, D. R., and O'Keefe, J., 2000. New England Forests Through Time. Insights from the Harvard Forest Dioramas. Harvard University Press

Goher, M.E., Farhat, H.I., Abdo, M.H., Salem, S.G., 2014b. Metal Pollution Assessment in The Surface Sediment of Lake Nasser, Egypt. Egypt. Aquat. Res. 40:213–224.

Goher, M.E., Hassan, A.M., Abdel-Moniem, I.A., Fahmy, A.H., El-Sayed, S.M., 2014a. Evaluation of Surface Water Quality and Heavy Metal Indices of Ismailia Canal, Nile River,

Egypt. Egypt. Aquat. Res. 40:225–233.

Guth, A., and Wood, J., 2013. Geological Map of the Southern Kenya Rift.

Hashim, M.A., Mukhopadhyay, S., Sahu, S.J., Sengupta, B., 2011. Remediation Technologies for Heavy Metal Contaminated Groundwater. Environ. Manage. 92(10):2355–2388.

Heller, P.L., Peter, E.B., Humphrey, N.F., et al., 2001. Paradox of Downstream Fining and Weathering-Rind Formation in the Lower Hoh River, Olympic Peninsula, Washington. Geology. 29(11):971-974

Jansen, L.J.M., and Di Gregorio, A., 2002. Parametric Land-Cover and Land-Use Classifications as Tools for Environmental Change Detection. Agriculture. Ecosystems & Environment. 91:89–100

Krissek, L.A, & Kyle, P.R., 2001. Geochemical Indicators of Weathering, Cenozoic Palaeoclimates, and Provenance from Fine-Grained Sediments in CRP-2/2A, Victoria Land Basin, Antarctica. Terra Antartica. 8(4)

Li, C., Yang, S.Y., 2010. Is Chemical Index of Alteration a Reliable Proxy for Chemical Weathering in Global Drainage Basins? Sci. 310: 111–127

Lohani, M.B., Singh, S., Rupainwa, D., Dhar, D.N., 2008. Seasonal Variations of Heavy Metal Contamination in River Gomti of Lucknow City Region. Environ. Monit. Assess. 147 (1): 253–263.

Ministry of Environment and Mineral Resources, Kenya, 2009. Nairobi River Basin Rehabilitation Program. 20th Anniversary of the adoption of the Basel Convention. http://www.basel.int/Portals/4/Basel%20Convention/docs/convention/XX%20Anniversary/Press%20kit/Kenya%20Project%20leaflet.pdf

McCarthy, M.J., Muller-Karger, F.E., Otis, D.B., Mendez-Lazaro, P., 2018. Impacts of 40 years of land cover change on water quality in Tampa Bay, Florida. Cogent Geoscience. 4

Nairobi City Water & Sewerage Company, 2011. Waste Water Treatment. Retrieved 6 November 2011.

Nesbitt, H.W., Young, G.M., 1989. Formation and Diagenesis of Weathering Profiles. Geol. 97: 129–147

Niu, L., Yang. F., Xu, C., Yang, H., Liu, W., 2013. Status of Metal Accumulation in Farmland Soils Across China: From Distribution to Risk Assessment. Env. Pol. 176:55-62

Nriagu, J.O., Pacyna, J.M., 1988. Quantitative Assessment of Worldwide Contamination of Air, Water and Soils by Trace Metals. Nature. 333:134–139

Panasiuk, O., Hedstrom, A., Marsalek, J., Ashley, M.M., Viklander, M., 2015. Contamination of Stormwater by Wastewater: A Review of Detection Methods. Environ. Manag. 152:241–250.

Potter, P.E., Maynard, J.B., Depetris, P.J., 2005. Mud and Mudstones. Berlin. Springer 157–174

Price, J.R., and Velbel, M.A., 2003. Chemical Weathering Indices Applied to Weathering Profiles Development on Heterogeneous Felsic Metamorphic Parent Rocks. Chem. Geol. 202:397-416

Roddaz, M., Viers, J., Brusset, S., et al., 2006. Controls on Weathering and Provenance in The Amazonian Foreland Basin: Insights from Major and Trace Element Geochemistry of Neogene Amazonian Sediments. Chem Geol, 226:31–65

Saggerson, E.P., 1991. Geology of the Nairobi Area. Kenya Mines and Geological Dept. issue 98.

Saha, N., Rahman, M.S., Jolly, Y., Rahman, A., Sattar, M.A., Hai, M.A., 2016. Spatial Distribution and Contamination Assessment of Six Heavy Metals in Soils and Their Transfer into Mature Tobacco Plants in Kushtia District, Bangladesh. Environ. Sci. Pollut. Res. 23:3414-3426.

Savichtcheva, O., Okabe, S., 2006. Alternative Indicators of Fecal Pollution: Relations with Pathogens and Conventional Indicators, Current Methodologies for Direct Pathogen Monitoring and Future Application Perspectives. Water Res. 40:2463–2476.

Schueler, T., 1994. The Importance of Imperviousness. Watershed Protection Techniques. 1(3):100-111

Shabnam, N., Sharmila, P., Govindjee, Kim, H., & Pardha-Saradhi, P., 2017. Differential Response of Floating and Submerged Leaves of Longleaf Pondweed to Silver Ions. Frontiers in Plant Science. *8:*1052.

Shao, J.Q., Yang, S.Y., 2012. Does Chemical Index of Alteration (CIA) Reflects Silicate Weathering and Monsoonal Climate in The Changjiang River Basin? Chin Sci Bull. 57:1178–1187

Singare, P.U., Mishra, R.M., Trivedi, M.P., 2012. Sediment Contamination Due to Toxic Heavy Metals in Mithi River of Mumbai. Adv. Anal. Chem. 2 (3):14–24.

Sombroek, W.G., Pauw, B.J.A., 1980. Exploratory Soil Map of Kenya. Republic of Kenya. Ministry of Agriculture

Stemmer, K.L., 1976. Pharmacology and Toxicology of Heavy Metals: Antimony. Pharmacology and Therapeutics Part A. 1:157–160

Steininger, M.K., 1996. Tropical Secondary Forest Regrowth in The Amazon: Age, Area and Change Estimation with Thematic Mapper Data. Int. J. Remote Sensing. 17:9-27

Tallon, P., Magajna, B., Lofranco, C., Leung, K., 2005. Microbial Indicators of Fecal Contamination in Water: A Current Perspective. Water Air Soil Pollut. 166:139–166

Tong, S.T.Y., and Chen, W.L., 2002. Modeling the Relationship Between Land-use and Surface Water Quality. Environmental Management. 4:377-393

Tromboni, F., and Dodds, W.K., 2017. Relationships Between Land Use and Stream Nutrient Concentrations in a Highly Urbanized Tropical Region of Brazil: Thresholds and Riparian Zones. Environmental Management. 60:30-40

Turner, C.L., Seastedt, T.R., and Dyer, M.I., 1993. Maximization of Above Ground Grassland Production: The Role of Defoliation Frequency, Intensity, And History. Ecological Applications 3:175–186

United Nations 2017. 72nd Session of the UN General Assembly (UNGA 72)

USEPA, 2012. Edition of the Drinking Water Standards and Health Advisories. U. S. Environmental Protection Agency, Washington, DC.

USEPA, 2015. Review of Coliphages as Possible Indicators of Fecal Contamination for Ambient Water Quality. EPA Office of Water (820-R-15-098).

WHO, 2006. Guidelines for Drinking-water: Incorporating First Addendum, 3rd ed. In: Recommendations, vol. 1. World Health Organization, Geneva, 515 pp.

Yang, S.Y., Jung, H. S., Li, C.X., 2004. Two Unique Weathering Regimes in The Changjiang and Huanghe Drainage Basins: Geochemical Evidence from River Sediments. Sediment Geol. 164:19–34

Zhang, L., Luo, X., Zeng, J., and Lui, S., 2015. An Effective and Recyclable Adsorbent for the Removal of Heavy Metal Ions from Aqueous System: Magnetic Chitosan/cellulose microspheres. Biortech. 194:403-406

APPENDICES

Appendix A Inorganic Element Data

Appendix A.1 Major oxides

ANALYSIS	WEI-21	ME-ICP06	ME-ICP06	ME-ICP06	ME-ICP06	ME-ICP06	ME-ICP06	ME-ICP06	ME-ICP06	ME-ICP06	ME-ICP06
SAMPLE	**Recvd Wt.**	**SiO_2**	**Al_2O_3**	**Fe_2O_3**	**CaO**	**MgO**	**Na_2O**	**K_2O**	**Cr_2O_3**	TiO_2	MnO
DESCRIPTION	**kg**	**%**	**%**	**%**	**%**	**%**	**%**	**%**	**%**	%	%
NR1	0.04	57.8	12.6	9.78	1.61	0.41	2.7	2.75	0.01	1.2	0.68
NR2	0.06	58.4	15.55	7.51	1.19	0.44	2.78	2.73	0.01	0.95	0.26
NR3	0.04	50	15.8	9.88	0.98	0.46	2.11	2.3	0.01	0.93	0.52
NR4	0.04	45.2	17.3	9.63	1.45	0.51	1.63	1.79	0.01	1.02	0.29
NR5	0.04	42	15.7	9	1.61	0.52	1.43	1.6	0.01	0.95	0.24
NR6	0.06	53.4	16.35	8.64	1.01	0.64	1.41	1.62	<0.01	0.93	0.36
NR7	0.04	55	16.9	9.44	0.49	0.2	2.96	2.82	<0.01	0.86	0.25
MR1	0.04	39.5	12.15	7.1	2.16	0.54	1.81	2.03	0.01	0.71	0.24
NR1 Copy	0.04	59.3	12.75	9.98	1.33	0.4	2.73	2.81	0.01	1.26	0.72
Hawaii Basalt	0.04	49.5	13.15	12.1	10.95	7.14	2.22	0.48	0.04	2.64	0.17

Appendix A.2 Major Oxides, LOI, Total, Carbon and Sulfur

ANALYSIS	ME-ICP06	ME-ICP06	ME-ICP06	OA-GRA05	TOT-ICP06	C-IR07	S-IR08
SAMPLE	P_2O5	SrO	BaO	LOI	Total	C	S
DESCRIPTION	%	%	%	%	%	%	%
NR1	0.41	0.01	0.1	9.24	99.3	2.42	0.12
NR2	0.17	0.01	0.06	9.62	99.68	1.27	0.13
NR3	0.52	0.01	0.09	16.25	99.86	4.67	0.08
NR4	0.59	0.01	0.04	19.95	99.42	5.68	0.28
NR5	0.77	0.01	0.04	24.6	98.48	7.81	0.47
NR6	0.11	0.01	0.06	14.45	98.99	1.06	0.02
NR7	0.14	<0.01	0.03	11	100.09	2.29	0.03
MR1	0.79	0.01	0.05	31.2	98.3	13.15	0.43
NR1 Copy	0.39	0.01	0.1	8.64	100.43	2.1	0.11
Hawaii Basalt	0.26	0.05	0.02	-0.61	98.11	0.04	0.02

Appendix A.3 Geochemical Analysis

ANALYSIS	ME-MS81	ME-MS81	ME-MS81	ME-MS81	ME-MS81	ME-MS81	ME-MS81	ME-MS81	ME-MS81	ME-MS81	ME-MS81
SAMPLE	Ba	Ce	Cr	Cs	Dy	Er	Eu	Ga	Gd	Ge	Hf
DESCRIPTION	ppm	ppm	ppm	ppm	ppm	ppm	ppm	ppm	ppm	ppm	ppm
NR1	797	413	90	1.07	12.4	7.46	2.77	25.5	12.2	<5	16.3
NR2	556	237	50	1.81	9.67	5.91	2.17	31.5	9.37	<5	19.5
NR3	783	538	70	1.78	17.3	10.05	3.27	33.3	17.1	<5	21.4
NR4	363	402	40	2.37	16.9	10.55	2.93	38	17	<5	26.4
NR5	324	368	40	2.16	15.95	9.55	2.75	34.3	15.8	<5	23.4
NR6	548	769	30	2.18	25.5	15.2	4.69	35.7	25.3	<5	23.4
NR7	227	499	30	1.98	24.1	15.15	2.88	45	21.9	<5	41.4
MR1	443	332	50	1.4	11.3	6.36	2.28	26.1	11.2	<5	18
NR1 Copy	841	445	80	0.98	12.15	7.34	2.7	25.9	12.6	<5	16.8
Hawaii Basalt	132	36.7	320	0.09	5.27	2.51	1.96	20.6	5.99	<5	4.3

Appendix A.4 Geochemical Analysis

ANALYSIS	ME-MS81	ME-MS81	ME-MS81	ME-MS81	ME-MS81	ME-MS81	ME-MS81	ME-MS81	ME-MS81	ME-MS81	ME-MS81
SAMPLE	Ho	La	Lu	Nb	Nd	Pr	Rb	Sm	Sn	Sr	Ta
DESCRIPTION	ppm	ppm	ppm	ppm	ppm	ppm	ppm	ppm	ppm	ppm	ppm
NR1	2.56	139	0.99	193	87.5	26.1	70.5	14.8	19	113	9.3
NR2	1.96	103.5	0.82	225	66.7	20.1	78.1	11.55	9	94.4	11
NR3	3.52	214	1.31	232	126	37.4	86.5	21.4	80	87.8	11.8
NR4	3.49	185	1.41	278	116	34.4	92.8	20.5	10	83.2	14.6
NR5	3.33	176	1.27	255	108.5	32.2	85.5	19.3	8	87.4	13.1
NR6	5.06	314	1.92	241	181	54.1	91.1	30.5	7	76.6	12.4
NR7	4.99	278	2.37	415	168	51.2	103.5	29	12	34.7	21
MR1	2.25	136	0.9	194.5	84.4	25.2	77.4	14.25	9	123.5	9.7
NR1 Copy	2.47	141.5	0.99	196	90.2	26.7	70.8	15.5	20	109.5	9.6
Hawaii Basalt	0.94	14.9	0.27	18.6	23.5	5.15	8.8	5.86	2	397	1.1

Appendix A.5 Geochemical Analysis

ANALYSIS	ME-MS81	ME-MS81	ME-MS81	ME-MS81	ME-MS81	ME-MS81	ME-MS81	ME-MS81	ME-MS81	ME-MS42	ME-MS42
SAMPLE	Tb	Th	Tm	U	V	W	Y	Yb	Zr	As	Bi
DESCRIPTION	ppm	ppm	ppm	ppm	ppm	ppm	ppm	ppm	ppm	ppm	ppm
NR1	2.04	17.65	1.06	3.99	30	3	67.7	6.68	769	4.5	0.14
NR2	1.56	22.3	0.9	5.18	23	4	53.7	5.54	909	1.9	0.17
NR3	2.89	24.8	1.49	5.43	37	4	94.8	9.02	997	22.5	0.42
NR4	2.83	29.3	1.54	5.12	34	5	95.7	9.78	1210	3.5	0.31
NR5	2.56	26.9	1.41	4.64	31	4	88.4	8.85	1075	3.4	0.25
NR6	4.17	27.6	2.17	5.4	35	4	145.5	13.05	1070	2.9	0.13
NR7	3.92	44.6	2.34	6.11	22	5	127	15.8	1890	3.3	0.15
MR1	1.91	20.6	0.94	4.45	25	4	60.9	6.03	850	4.5	0.45
NR1 Copy	2.02	16.8	1.09	3.87	32	3	67.2	6.83	786	4.2	0.13
Hawaii Basalt	0.9	1.34	0.32	0.41	350	1	24.4	1.84	174	0.3	0.01

Appendix A.6 Geochemical Analysis

ANALYSIS	ME-MS42	ME-MS42	ME-MS42	ME-MS42	ME-MS42	ME-MS42	ME-MS42	ME-4ACD81	ME-4ACD81	ME-4ACD81
SAMPLE	Hg	In	Re	Sb	Se	Te	Tl	Ag	Cd	Co
DESCRIPTION	ppm	ppm	ppm	ppm	ppm	ppm	ppm	ppm	ppm	ppm
NR1	0.219	0.082	0.001	1.85	0.2	0.04	0.46	0.5	<0.5	10
NR2	0.076	0.111	<0.001	0.65	<0.2	0.01	0.25	0.5	<0.5	7
NR3	0.564	0.114	<0.001	187.5	3.4	0.07	0.56	3.9	0.7	16
NR4	0.107	0.159	0.001	0.77	0.3	0.03	0.83	<0.5	<0.5	10
NR5	0.082	0.149	0.001	0.77	0.6	0.03	0.84	<0.5	<0.5	9
NR6	0.03	0.144	0.001	0.22	<0.2	0.02	0.37	<0.5	<0.5	13
NR7	0.044	0.191	0.001	0.41	<0.2	0.05	0.46	<0.5	<0.5	7
MR1	0.344	0.093	<0.001	1.52	0.4	0.02	0.55	0.8	0.6	7
NR1 Copy	0.17	0.076	<0.001	2.45	<0.2	0.04	0.46	<0.5	<0.5	11
Hawaii Basalt	<0.005	0.011	0.001	0.13	0.3	0.01	<0.02	<0.5	<0.5	42

Appendix A.7 Geochemical Analysis

ANALYSIS	ME-4ACD81	ME-4ACD81	ME-4ACD81	ME-4ACD81	ME-4ACD81	ME-4ACD81	ME-4ACD81
SAMPLE	Cu	Li	Mo	Ni	Pb	Sc	Zn
DESCRIPTION	ppm	ppm	ppm	ppm	ppm	ppm	ppm
NR1	34	20	4	17	83	3	385
NR2	26	20	3	12	60	4	352
NR3	87	20	4	30	3400	4	614
NR4	38	30	4	21	52	6	499
NR5	34	30	4	19	44	5	490
NR6	10	20	3	20	33	5	161
NR7	11	30	4	11	44	5	467
MR1	66	20	4	16	65	3	628
NR1 Copy	32	20	4	15	97	3	384
Hawaii Basalt	125	<10	3	116	<2	29	102